Electronic Supplementary Information for "Hypoxia-activated dissociation of heteroleptic cobalt(III) complexes with functionalized 2,2'-bipyridines and a model anticancer drug esculetin"

by

Ekaterina Khakina,[ab] Igor Nikovskiy,[a] Kirill Spiridonov,[a] Valentin Novikov,[c] Evgenia Antoshkina,[a] Dzhuliia Dzhalilova,[d] Marina Diatroptova,[d] Alina Martyanova,[e] Alexey Rodionov[a] and Yulia V. Nelyubina*[a]

[a]A.N. Nesmeyanov Institute of Organoelement Compounds, Russian Academy of Sciences, 119334, Vavilova Str., 28, bld. 1, Moscow, Russia

[b]National Research University Higher School of Economics, Faculty of Chemistry, 101000, Vavilova Str., 7, Moscow, Russia

[c]Department de Quimica Inorganica and IN2UB, Universitat de Barcelona, Diagonal 647, 08028 Barcelona, Spain

[d]Avtsyn Research Institute of Human Morphology of Federal State Budgetary Scientific Institution "Petrovsky National Research Centre of Surgery", 1174183, Tsyurupy Str., Moscow, Russia

[e]Center for Precision Genome Editing and Genetic Technologies for Biomedicine, Pirogov Russian National Research Medical University, 117997, Ostrovityanova Str., 1, Moscow, Russia

*Corresponding Author. E-mail address: unelya@ineos.ac.ru

Supplementary Figures:

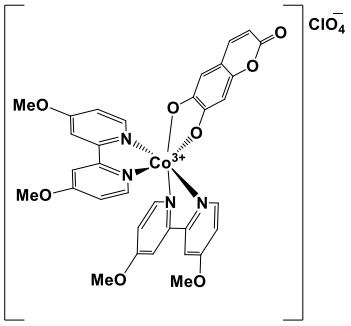

[Co(L^{OMe})$_2$(esc)]ClO$_4$

Chemical Formula: $C_{33}H_{28}ClCoN_4O_{12}$

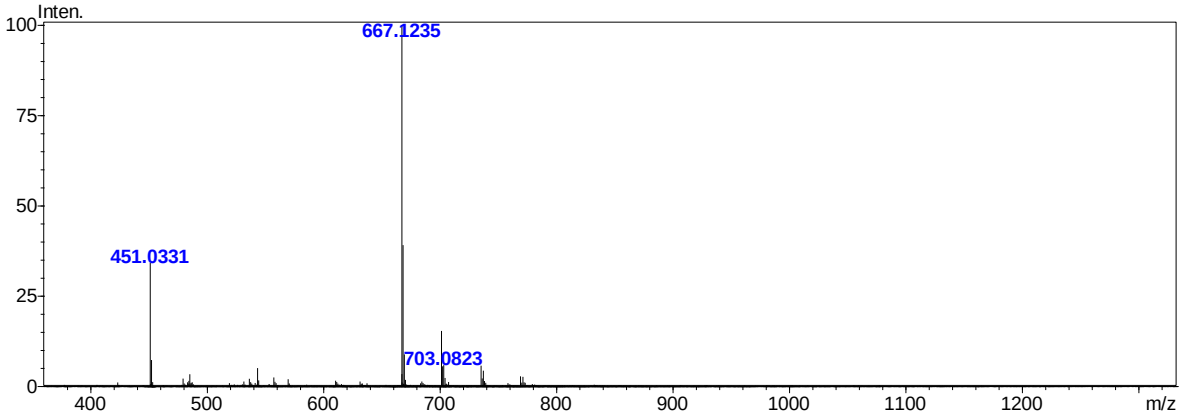

Figure S1. High-resolution mass spectrum (ESI) of [Co(**L**$^{\mathbf{OMe}}$)$_2$(**esc**)]ClO$_4$.

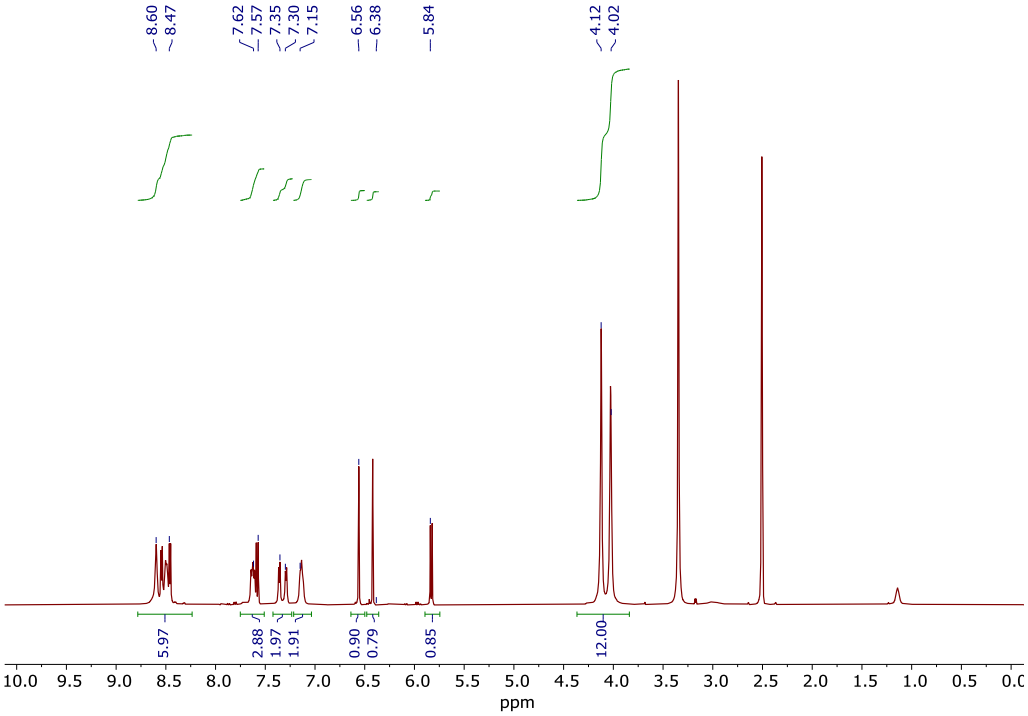

Figure S2. ^{1}H NMR spectrum of [Co(**L**$^{\mathbf{OMe}}$)$_2$(**esc**)]ClO$_4$ in DMSO-d$_6$.

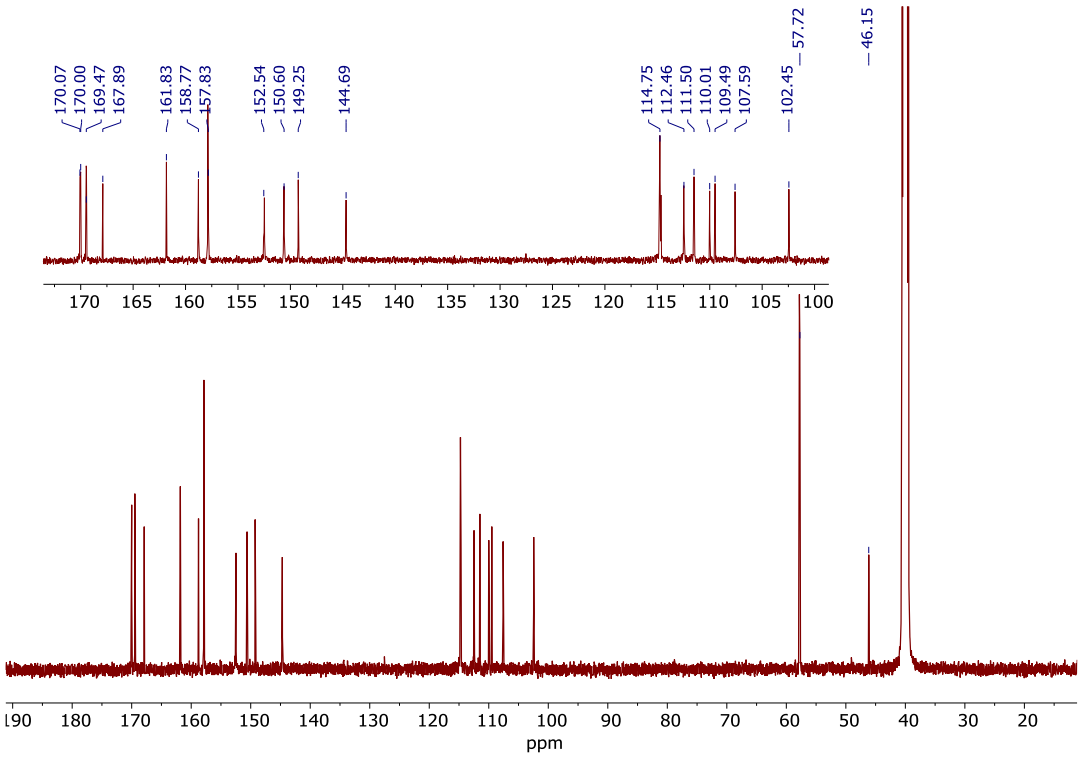

Figure S3. ^{13}C NMR spectrum of [Co(**L**$^{\mathbf{OMe}}$)$_2$(**esc**)]ClO$_4$ in DMSO-d$_6$.

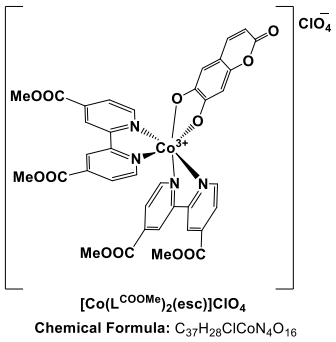

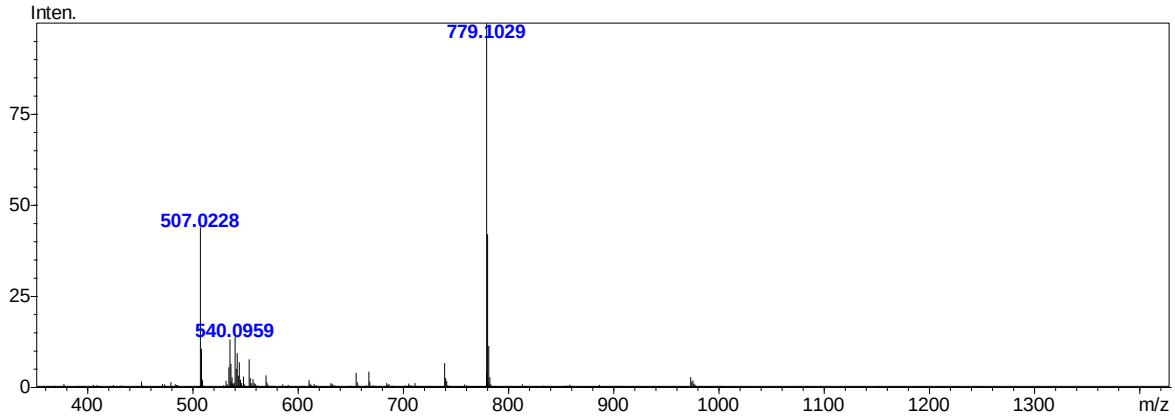

Figure S4. High-resolution mass spectrum (ESI) of [Co(**L**$^{\mathbf{COOMe}}$)$_2$(**esc**)]ClO$_4$.

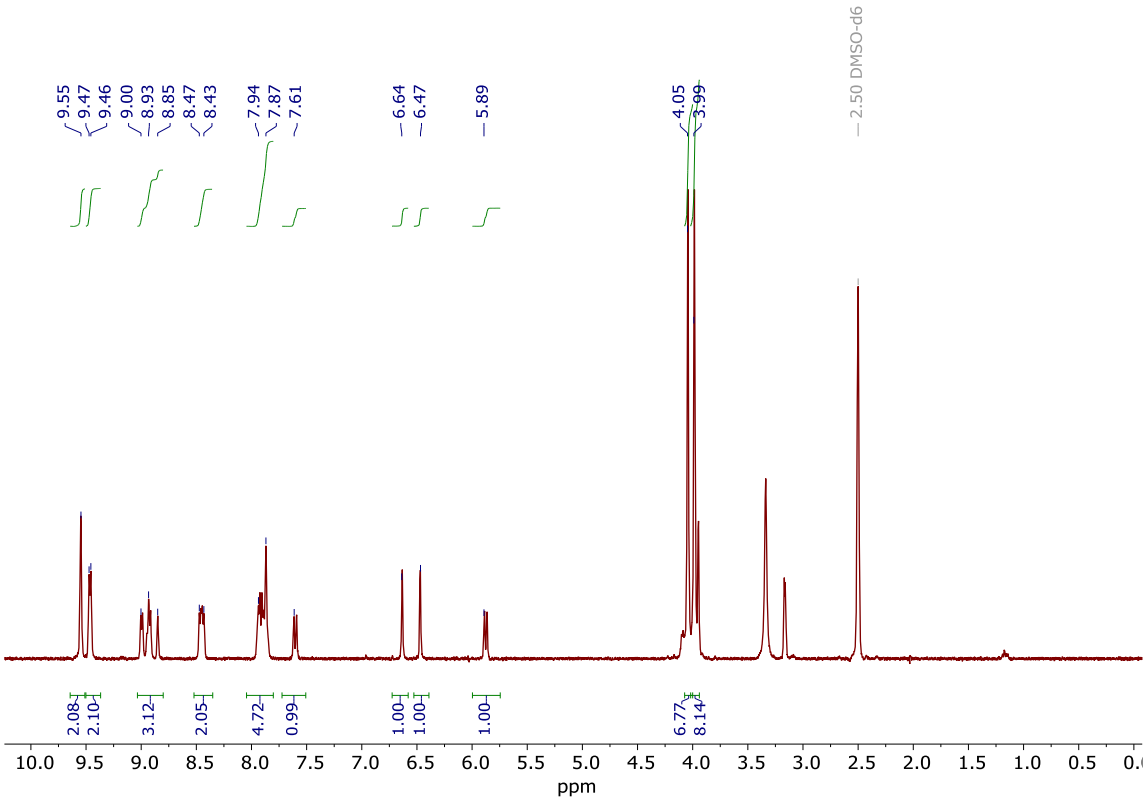

Figure S5. ^{1}H NMR spectrum of [Co(**L**$^{\mathbf{COOMe}}$)$_2$(**esc**)]ClO$_4$ in DMSO-d$_6$.

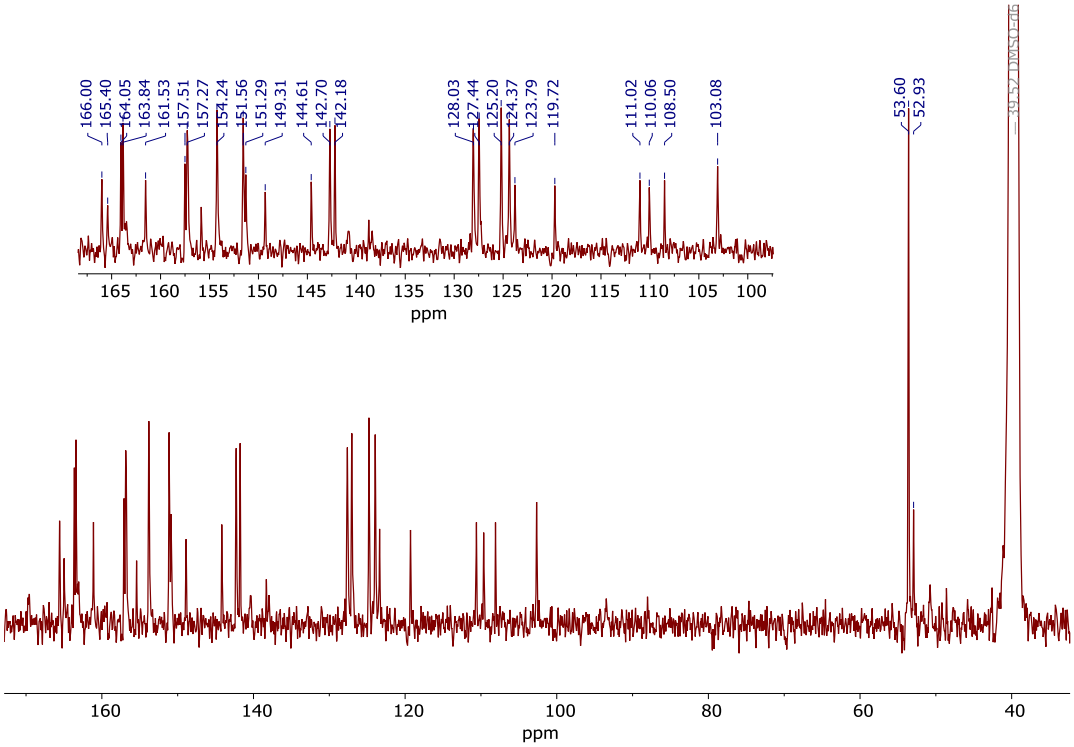

Figure S6. ^{13}C NMR spectrum of [**Co(L**$^{\mathbf{COOMe}}$)$_2$(**esc**)]ClO$_4$ in DMSO-d$_6$.

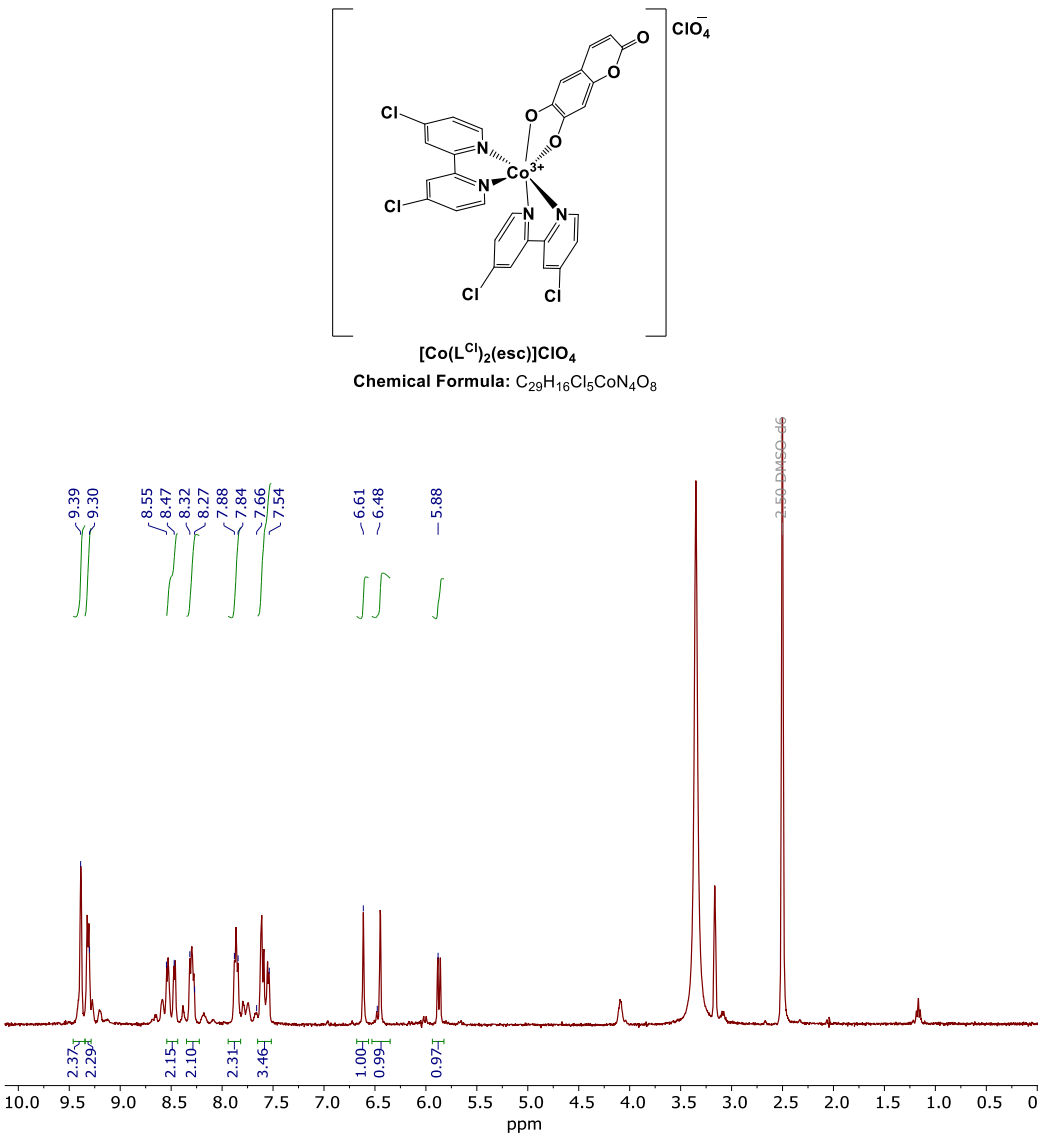

Figure S7. ^{1}H NMR spectrum of [Co(**L**$^{\mathbf{Cl}}$)$_2$(**esc**)]ClO$_4$ in DMSO-d$_6$.

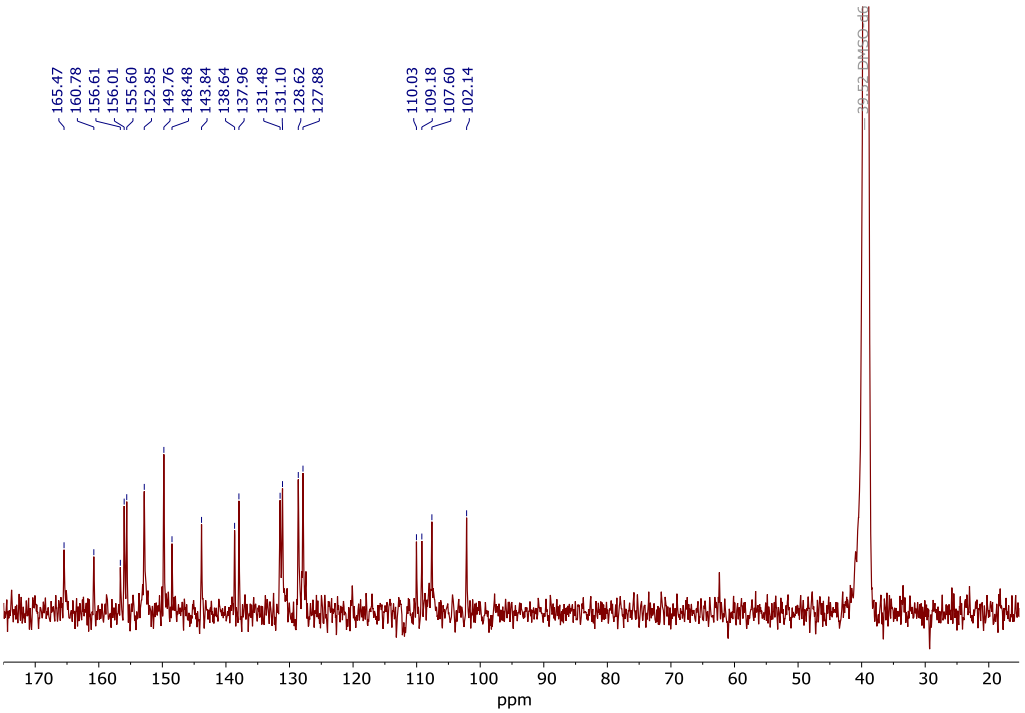

Figure S8. ^{13}C NMR spectrum of [Co(**L**^{Cl})$_2$(**esc**)]ClO$_4$ in DMSO-d$_6$.

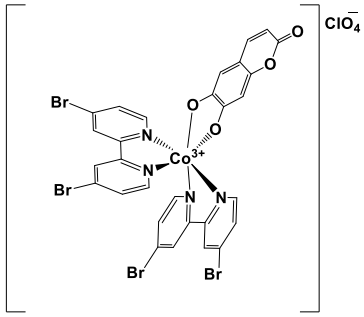

[Co(L^{Br})$_2$(esc)]ClO$_4$

Chemical Formula: $C_{29}H_{16}Br_4ClCoN_4O_8$

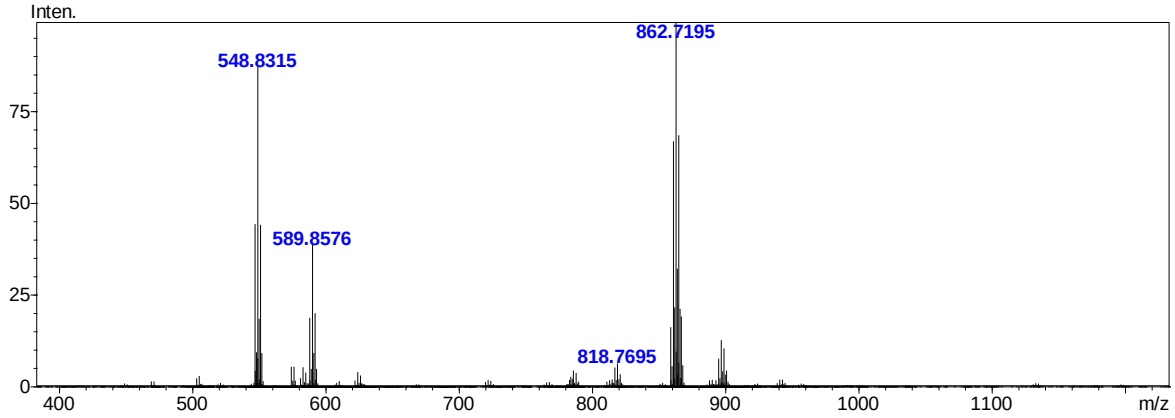

Figure S9. High-resolution mass spectrum (ESI) of [Co(**L**^{Br})$_2$(**esc**)]ClO$_4$.

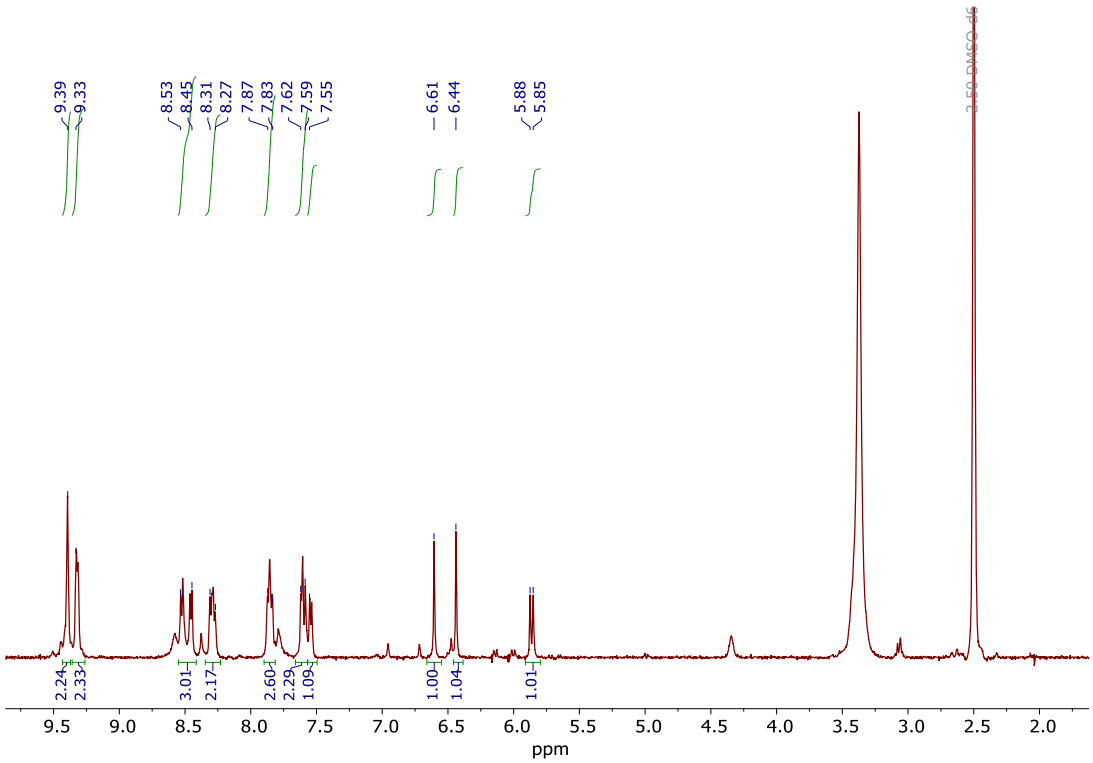

Figure S10. ^{1}H NMR spectrum of [Co(**L**$^{\mathbf{Br}}$)$_2$(**esc**)]ClO_4 in DMSO-d_6.

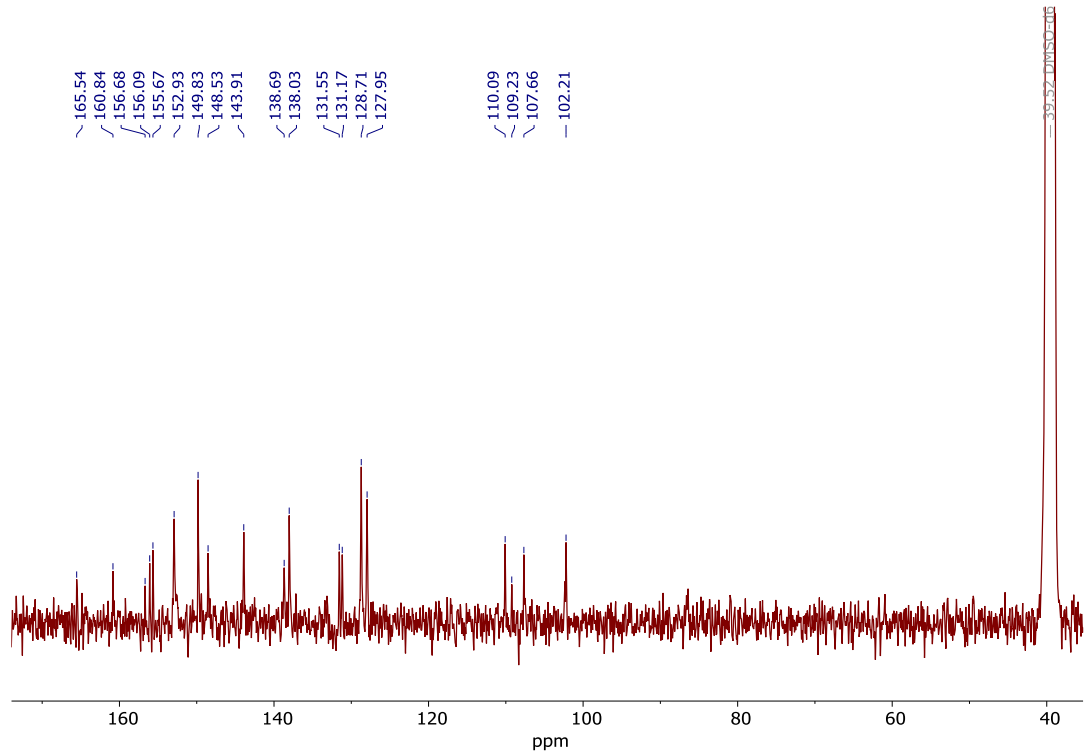

Figure S11. ^{13}C NMR spectrum of [Co(**L**$^{\mathbf{Br}}$)$_2$(**esc**)]ClO_4 in DMSO-d_6.

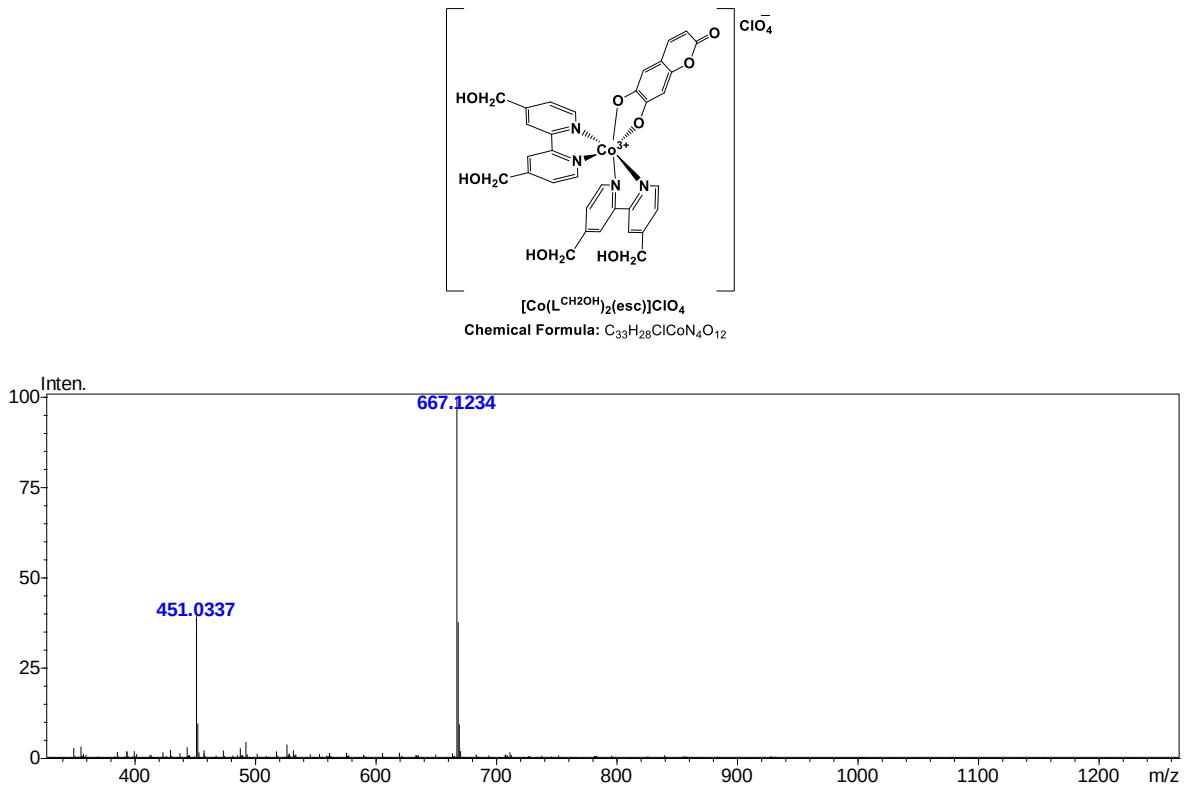

Figure S12. High-resolution mass spectrum (ESI) of [Co(**L**$^{\mathbf{CH_2OH}}$)$_2$(**esc**)]ClO$_4$.

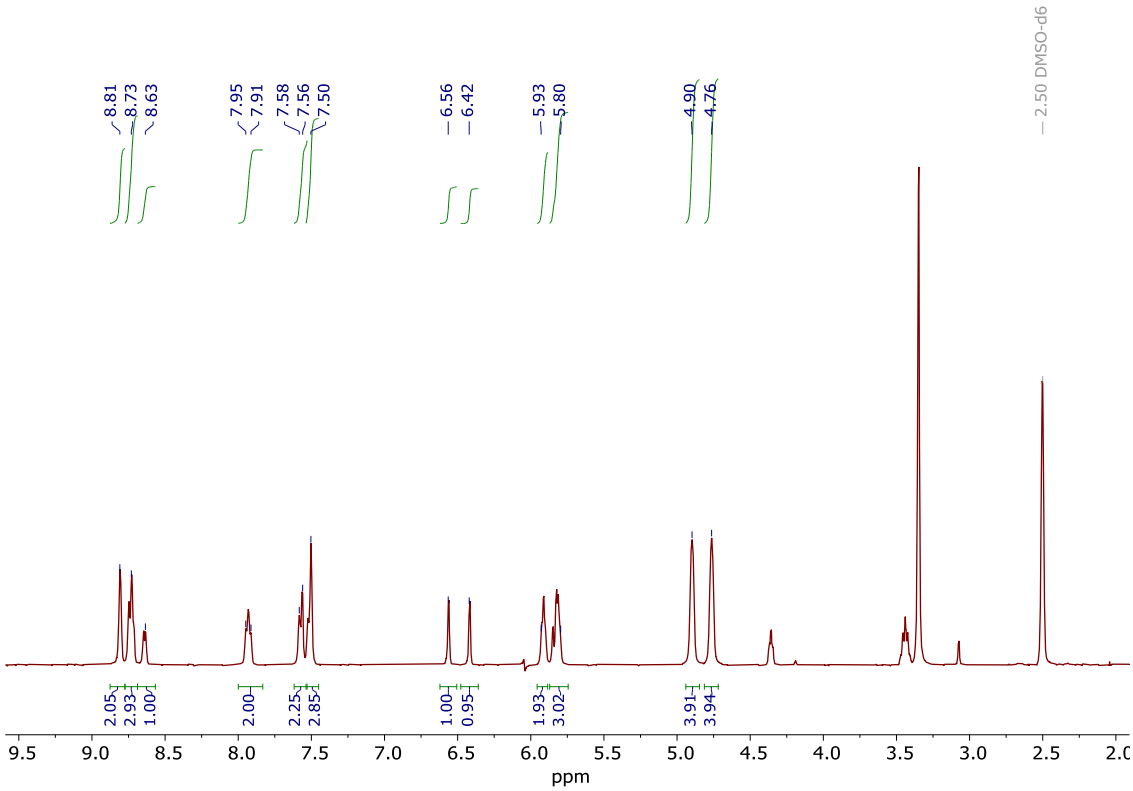

Figure S13. ^{1}H NMR spectrum of [Co(**L**$^{\mathbf{CH_2OH}}$)$_2$(**esc**)]ClO$_4$ in DMSO-d$_6$.

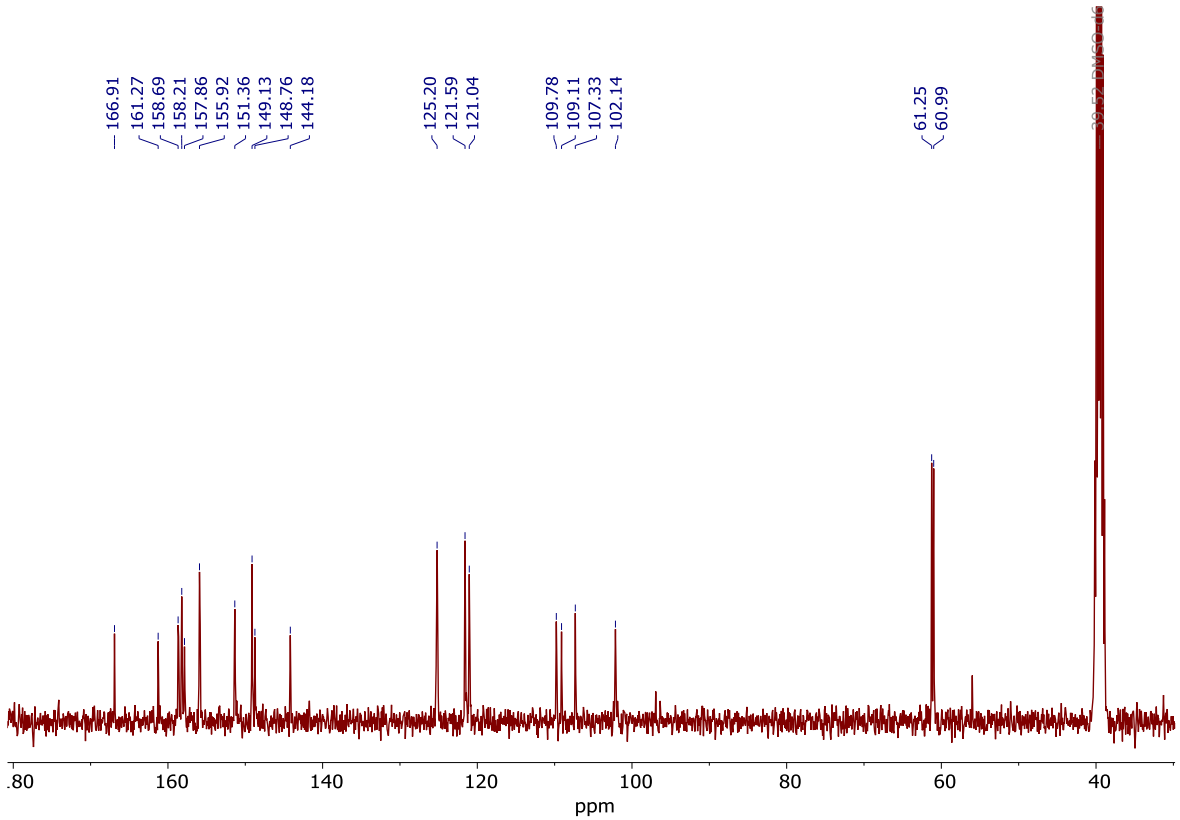

Figure S14. ^{13}C NMR spectrum of [Co($\mathbf{L^{CH_2OH}}$)$_2$(**esc**)]ClO$_4$ in DMSO-d$_6$.

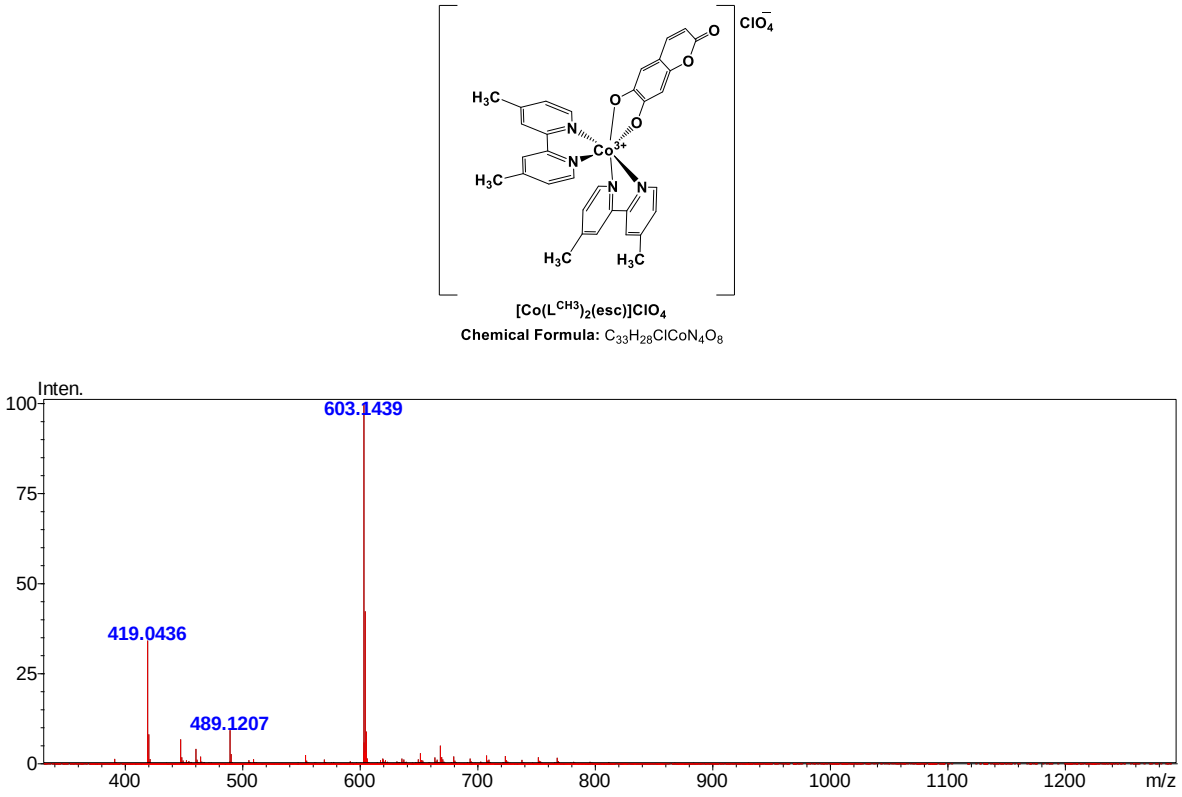

Figure S15. High-resolution mass spectrum (ESI) of [Co($\mathbf{L^{Me}}$)$_2$(**esc**)]ClO$_4$.

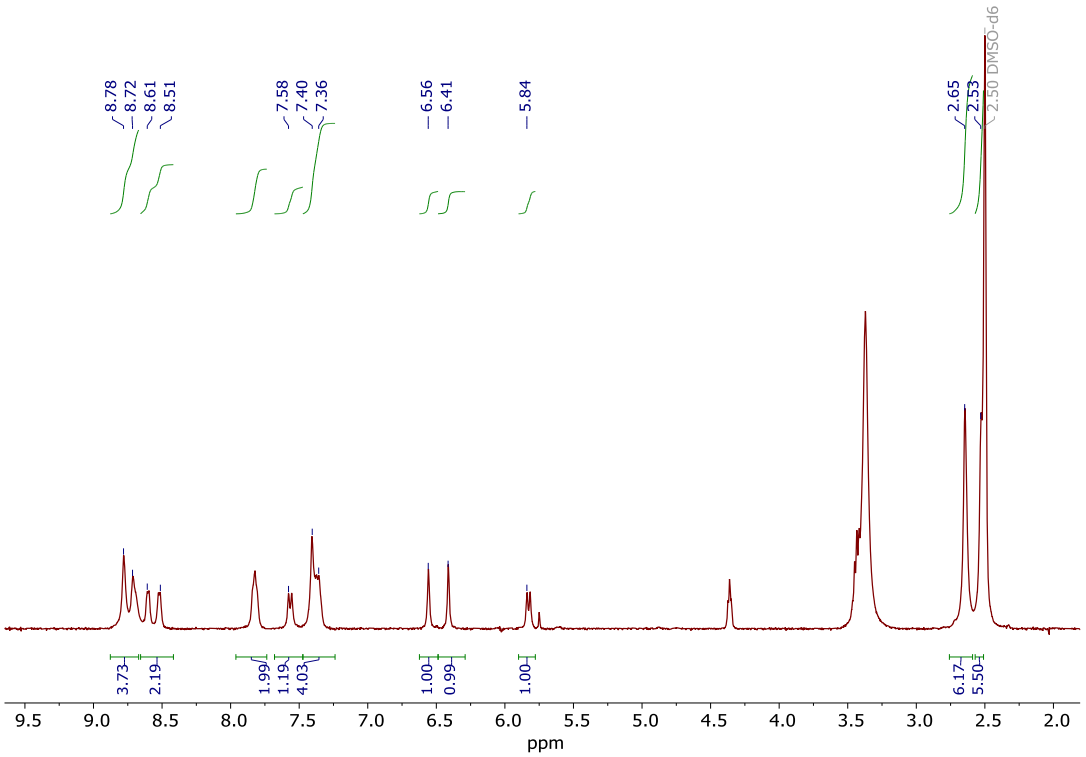

Figure S16. ^{1}H NMR spectrum of [Co(**L**$^{\mathbf{Me}}$)$_2$(**esc**)]ClO$_4$ in DMSO-d$_6$.

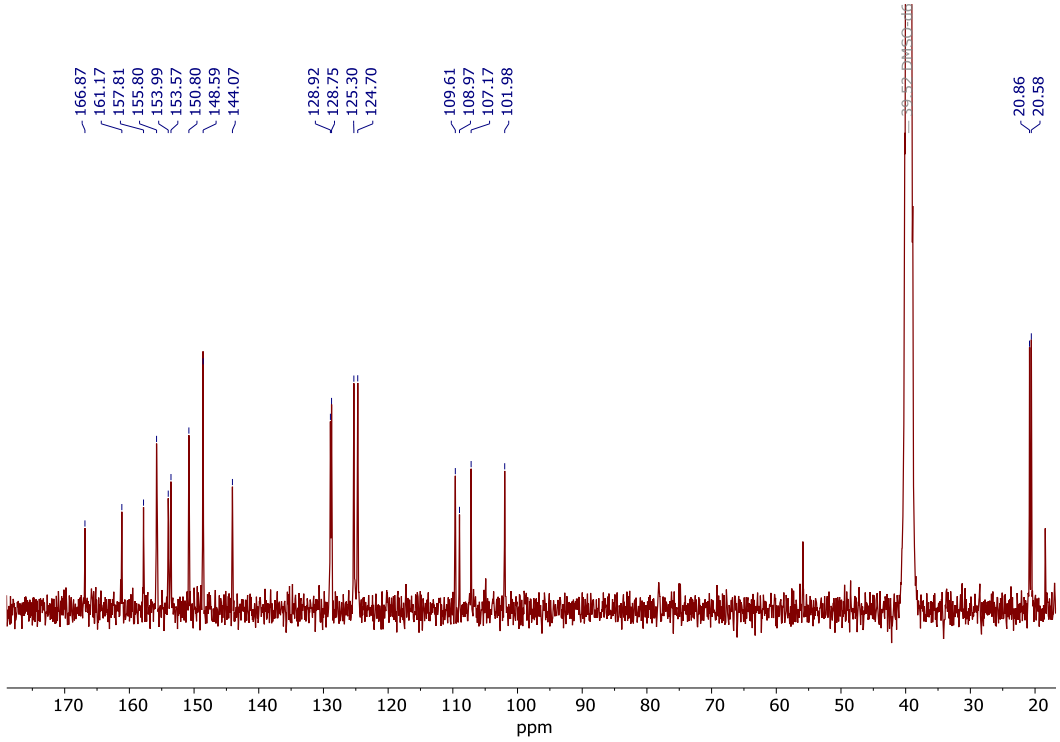

Figure S17. ^{13}C NMR spectrum of [**Co(L**$^{\mathbf{Me}}$)$_2$(**esc**)]ClO$_4$ in DMSO-d$_6$.

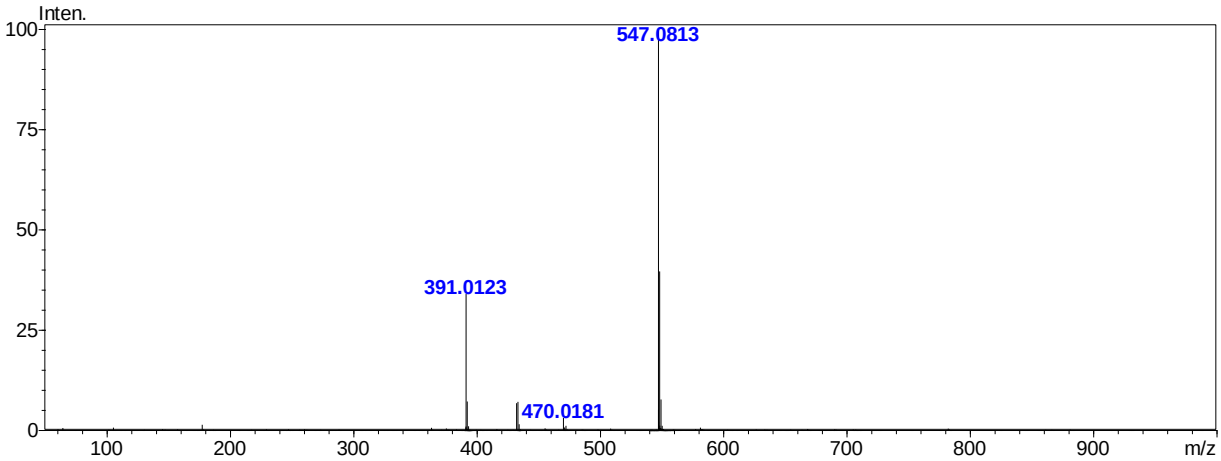

Figure S18. High-resolution mass spectrum (ESI) of [Co(**L**$^{\mathbf{H}}$)$_2$(**esc**)]ClO$_4$ featuring signals of ions [Co(**L**$^{\mathbf{H}}$)$_2$(**esc**)]$^+$ (m/z = 547.0813) and [Co(**L**$^{\mathbf{H}}$)(**esc**)]$^+$ (m/z = 391.0123).

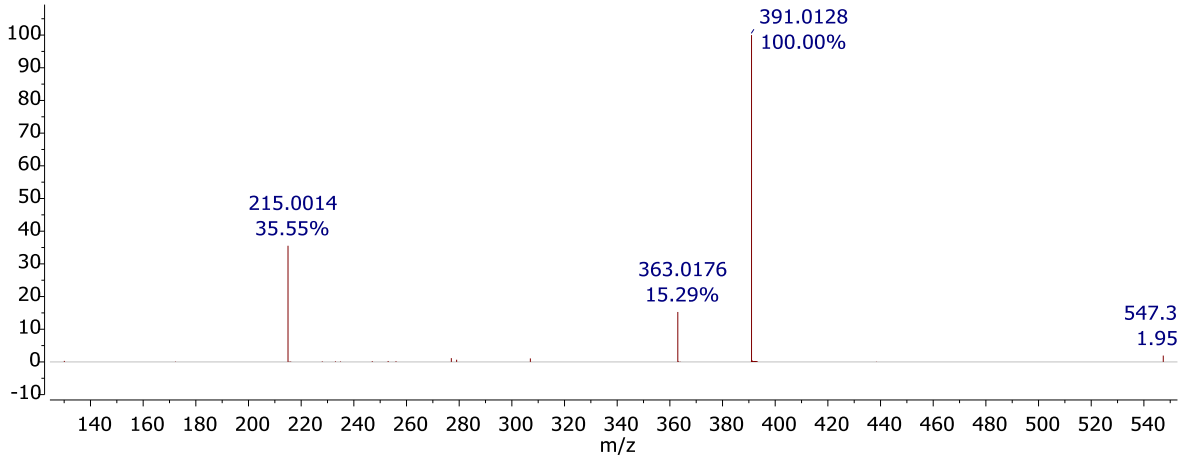

Figure S19. MS/MS spectrum featuring signals of ions [Co(**L**$^{\mathbf{H}}$)$_2$(**esc**)]$^+$ (m/z = 547.0813), [Co(**L**$^{\mathbf{H}}$)(**esc**)]$^+$ (m/z = 391.0128) and [Co(**L**$^{\mathbf{H}}$)]$^+$ (m/z = 215.0014); the collision energy was 35±17 V.

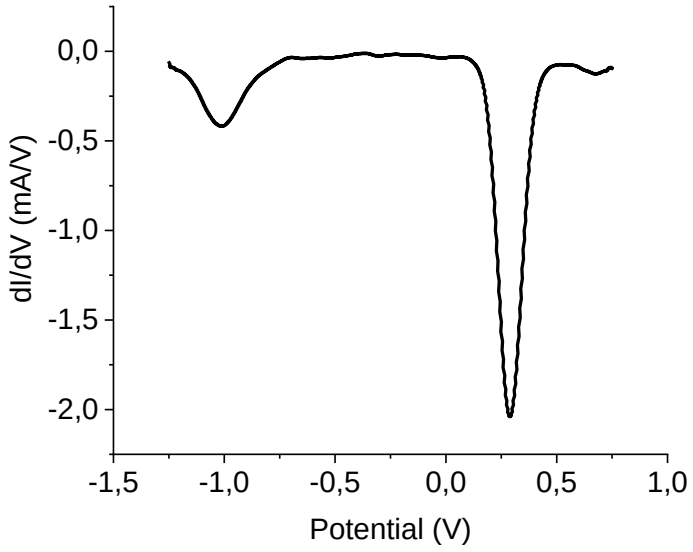

Figure S20. Differential pulse voltammogram (ν = 100 mV s^{-1}) of [Co(**L**$^{\mathbf{OMe}}$)$_2$(**esc**)]ClO_4 (2×10^{-3} mol/l) at 298 K in an acetonitrile-DMF mixture with 0.1 M [NBu_4][ClO_4] at a glassy carbon electrode.

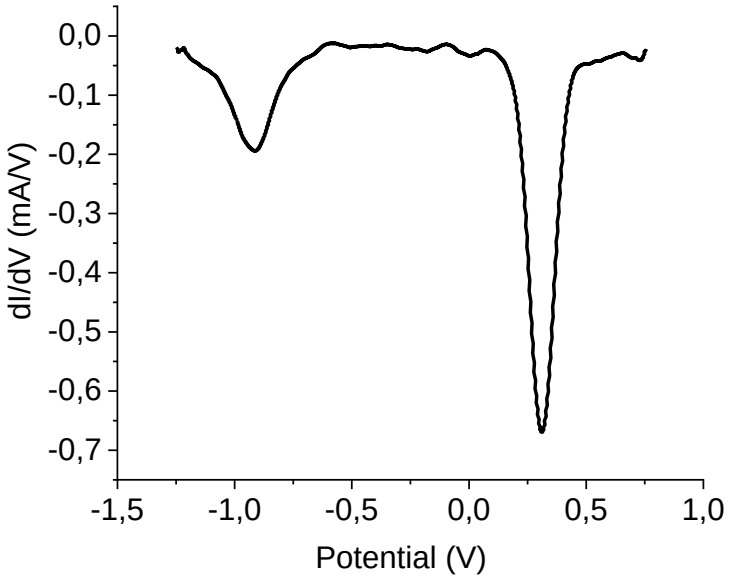

Figure S21. Differential pulse voltammogram (ν = 100 mV s^{-1}) of [Co(**L**$^{\mathbf{Me}}$)$_2$(**esc**)]ClO_4 (2×10^{-3} mol/l) at 298 K in an acetonitrile-DMF mixture with 0.1 M [NBu_4][ClO_4] at a glassy carbon electrode.

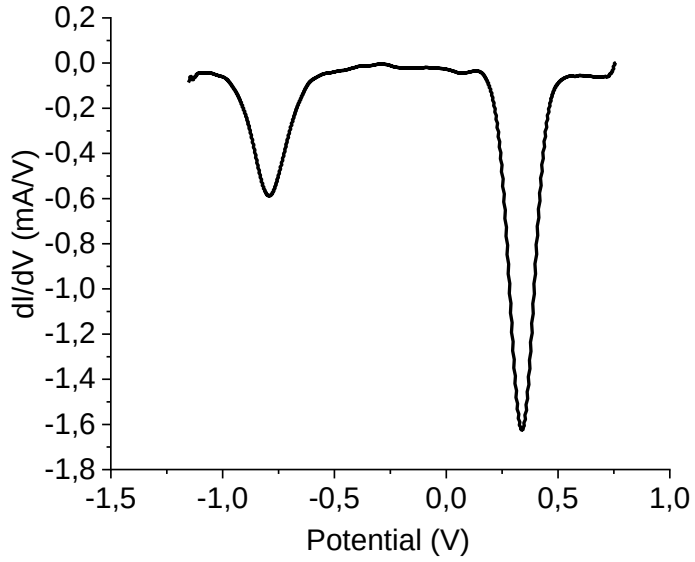

Figure S22. Differential pulse voltammogram (ν = 100 mV s^{-1}) of [Co(**L**$^{\mathbf{H}}$)$_2$(**esc**)]ClO_4 (2×10^{-3} mol/l) at 298 K in an acetonitrile-DMF mixture with 0.1 M [NBu_4][ClO_4] at a glassy carbon electrode.

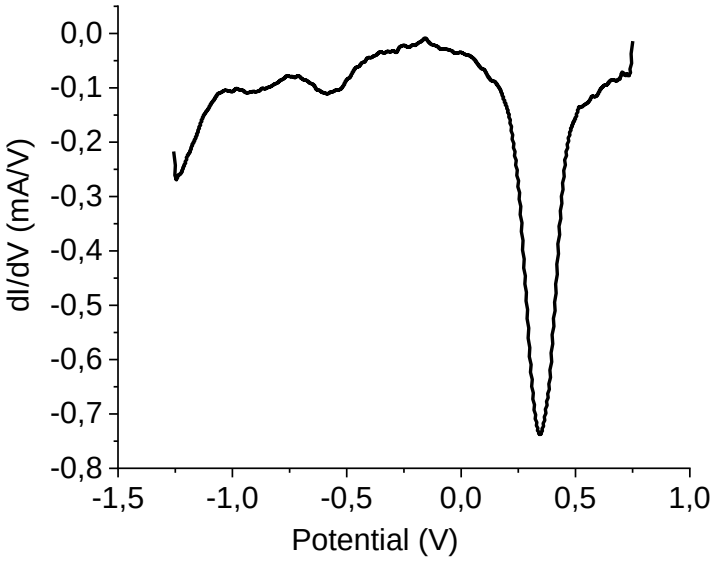

Figure S23. Differential pulse voltammogram (ν = 100 mV s^{-1}) of [Co(**L**$^{\mathbf{COOMe}}$)$_2$(**esc**)]ClO_4 (2×10^{-3} mol/l) at 298 K in an acetonitrile-DMF mixture with 0.1 M [NBu_4][ClO_4] at a glassy carbon electrode.

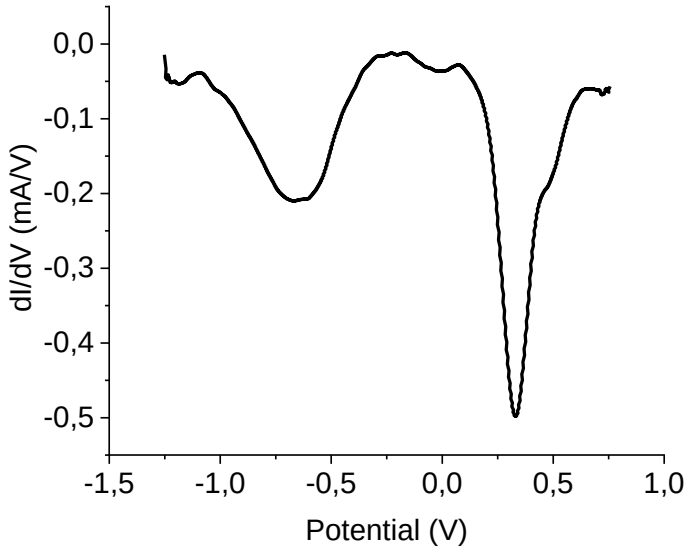

Figure S24. Differential pulse voltammogram (ν = 100 mV s^{-1}) of [Co(**L**$^{\mathbf{Cl}}$)$_2$(**esc**)]ClO_4 (2×10^{-3} mol/l) at 298 K in an acetonitrile-DMF mixture with 0.1 M [NBu_4][ClO_4] at a glassy carbon electrode.

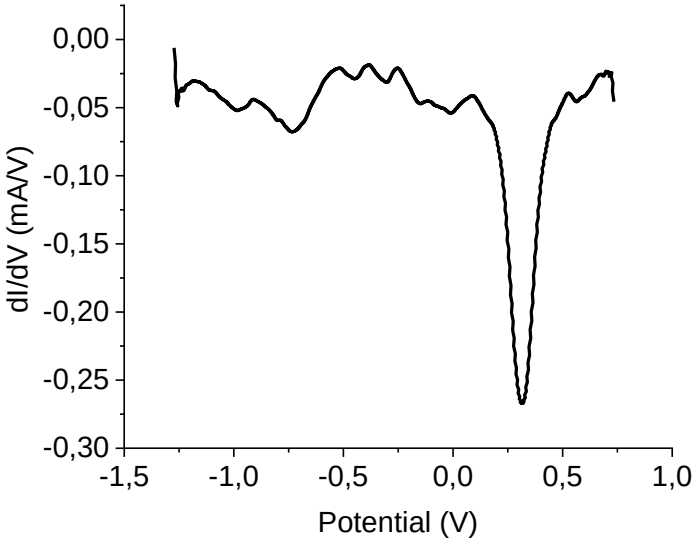

Figure S25. Differential pulse voltammogram (ν = 100 mV s^{-1}) of [Co(**L**$^{\mathbf{CH_2OH}}$)$_2$(**esc**)]ClO_4 (2×10^{-3} mol/l) at 298 K in an acetonitrile-DMF mixture with 0.1 M [NBu_4][ClO_4] at a glassy carbon electrode.

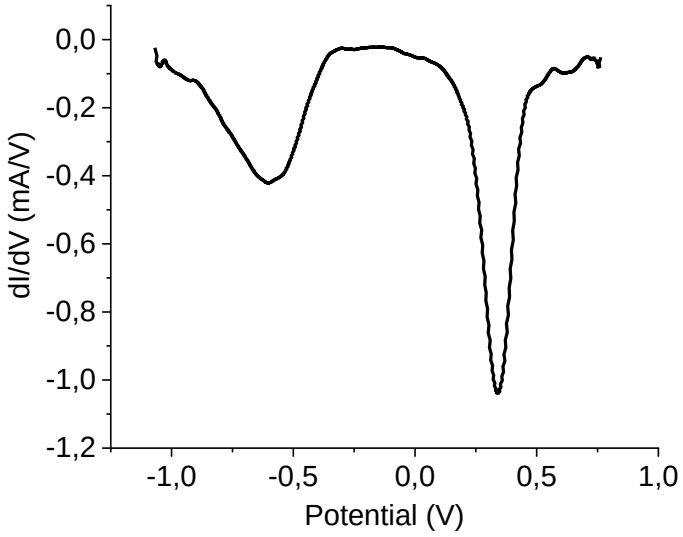

Figure S26. Differential pulse voltammogram (ν = 100 mV s^{-1}) of [Co(**L**$^{\mathbf{Br}}$)$_2$(**esc**)]ClO_4 (2×10^{-3} mol/l) at 298 K in an acetonitrile-DMF mixture with 0.1 M [NBu_4][ClO_4] at a glassy carbon electrode.

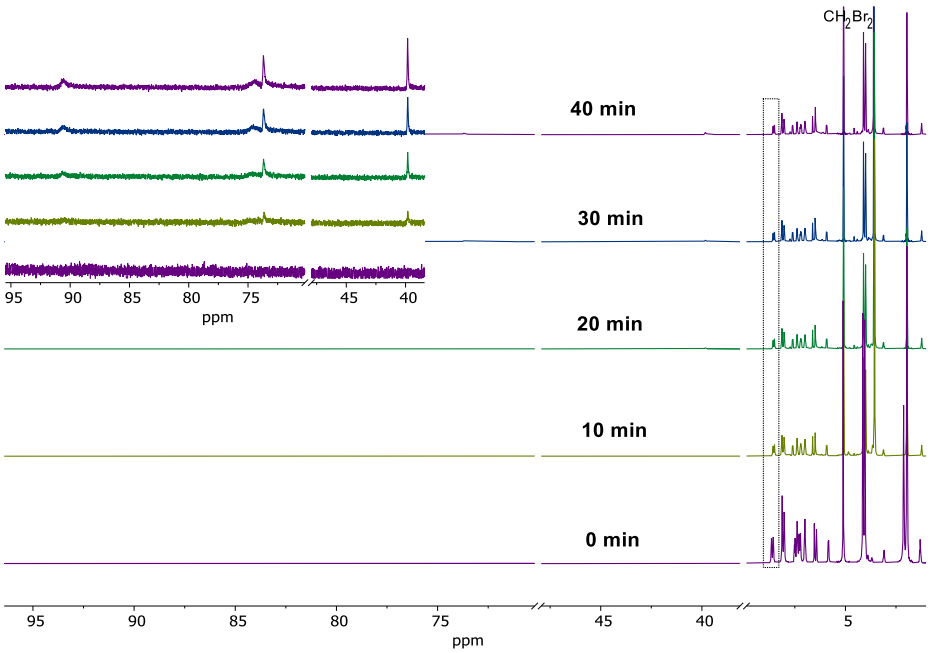

Figure S27. ^{1}H NMR spectra illustrating the dynamics of the reduction of the cobalt(III) complex [Co(**L**$^{\mathbf{OMe}}$)$_2$(**esc**)]ClO_4 by ascorbic acid under argon at 40°C. The inset shows the paramagnetic region of the spectra featuring four signals from the protons of this complex with their intensities increasing with the reduction time.

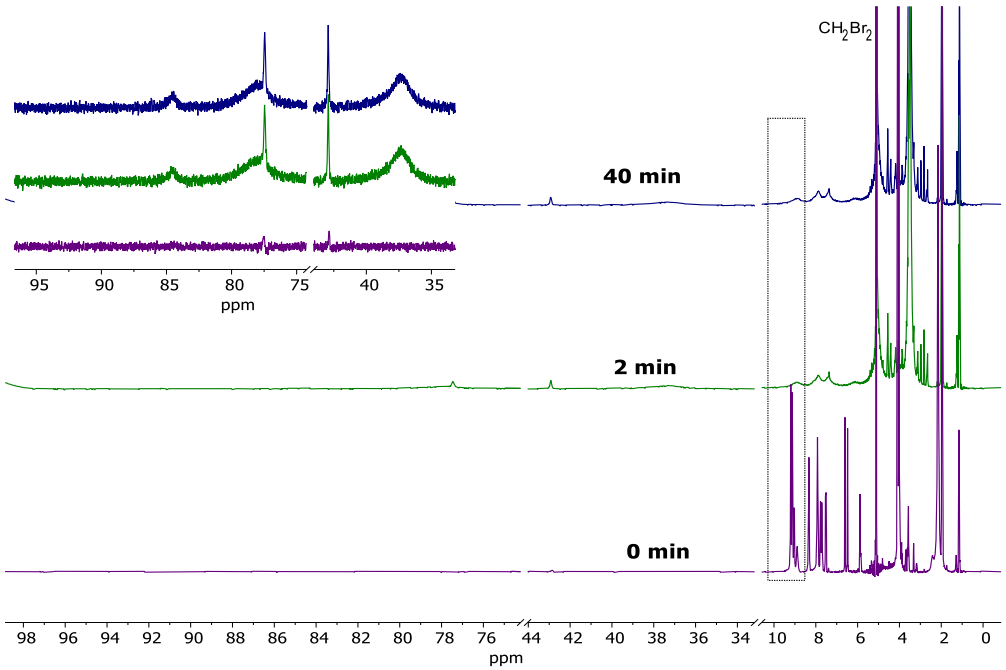

Figure S28. ^{1}H NMR spectra illustrating the dynamics of the reduction of the cobalt(III) complex [Co(**L**$^{\mathbf{COOMe}}$)$_2$(**esc**)]ClO$_4$ by ascorbic acid under argon at 40ºC. The inset shows the paramagnetic region of the spectra featuring four signals from the protons of this complex with their intensities increasing with the reduction time.

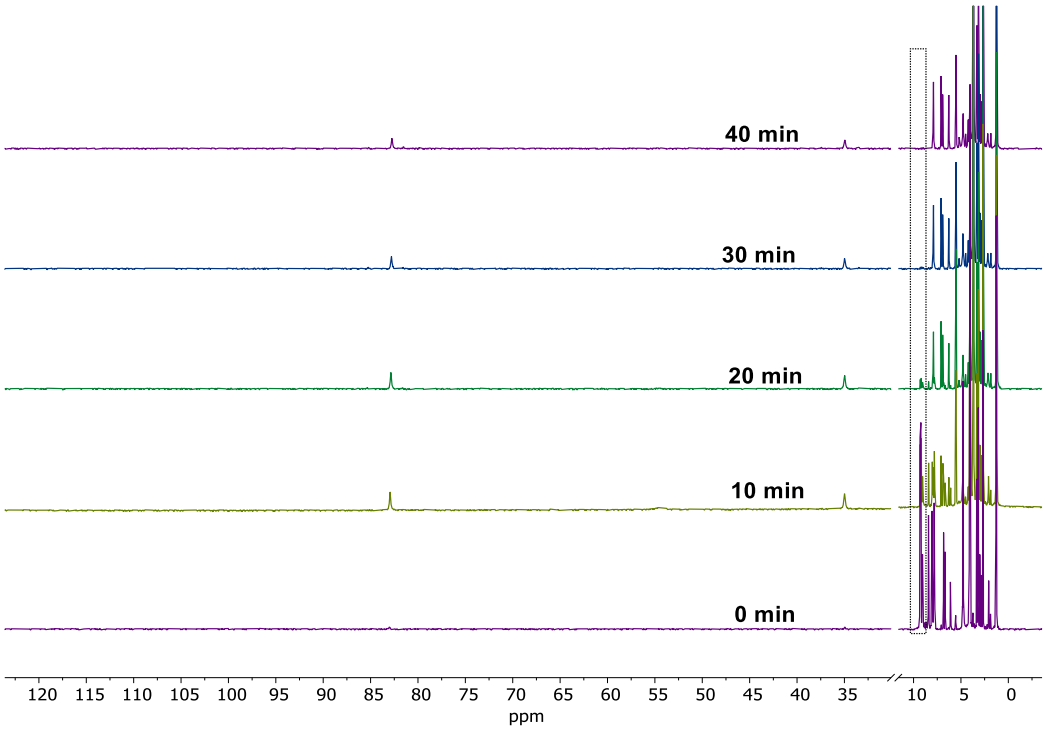

Figure S29. ^{1}H NMR spectra illustrating the dynamics of the reduction of the cobalt(III) complex [Co(**L**$^{\mathbf{COOMe}}$)$_2$(**esc**)]ClO$_4$ by ascorbic acid under argon at 20ºC.

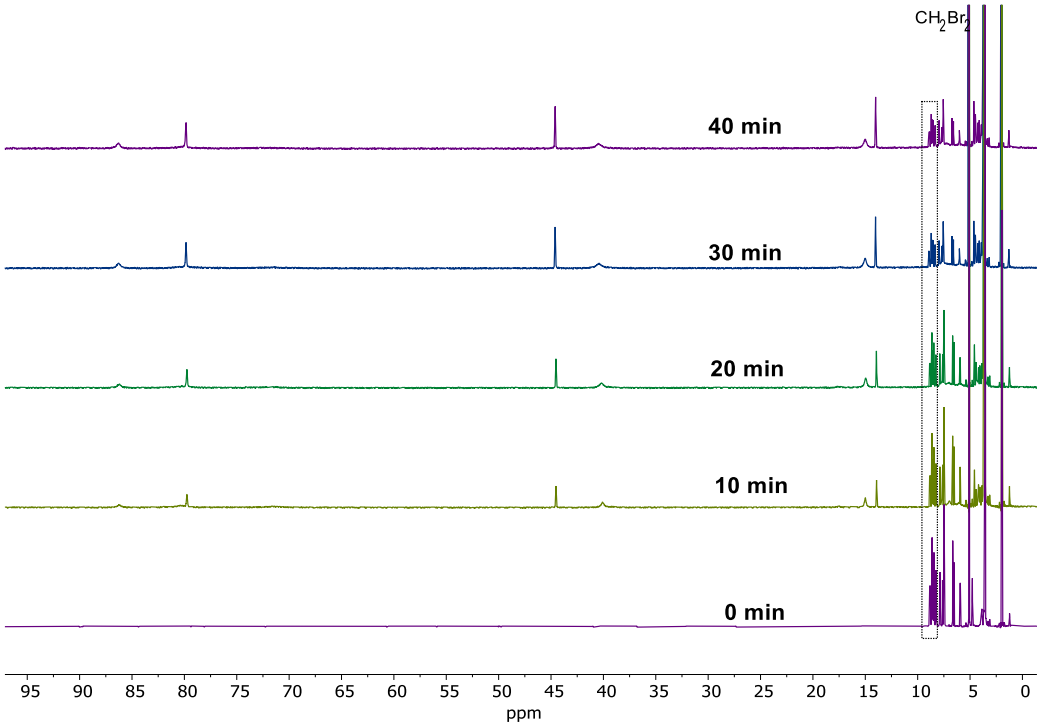

Figure S30. ^{1}H NMR spectra illustrating the dynamics of the reduction of the cobalt(III) complex [Co(**L**$^{\mathbf{H}}$)$_2$(**esc**)]ClO$_4$ by ascorbic acid under argon at 40°C.

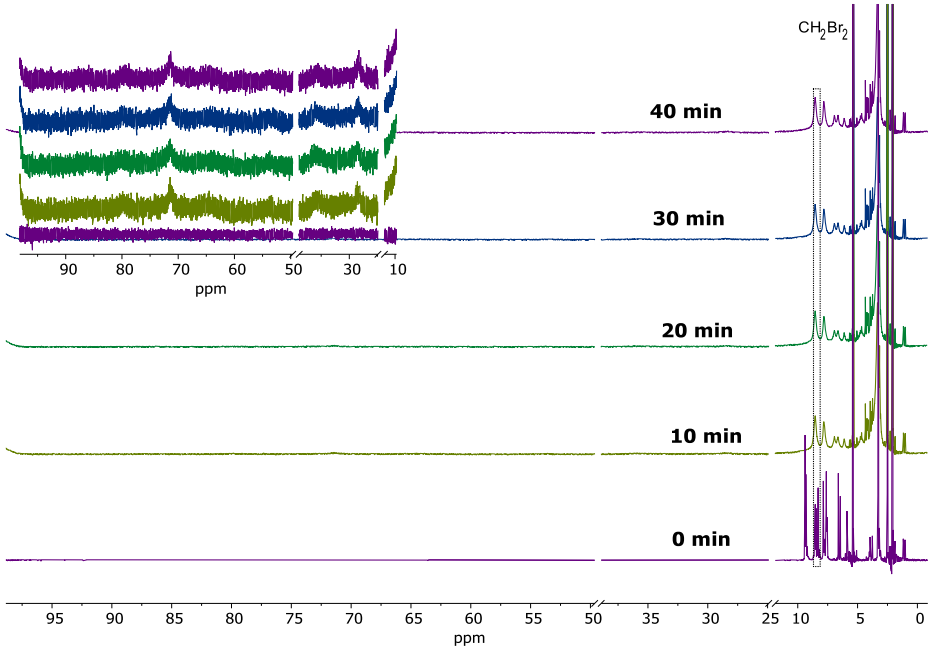

Figure S31. ^{1}H NMR spectra illustrating the dynamics of the reduction of the cobalt(III) complex [Co(**L**$^{\mathbf{Cl}}$)$_2$(**esc**)]ClO$_4$ by ascorbic acid under argon at 40°C. The inset shows the paramagnetic region of the spectra featuring three signals from the protons of this complex with their intensities increasing with the reduction time.

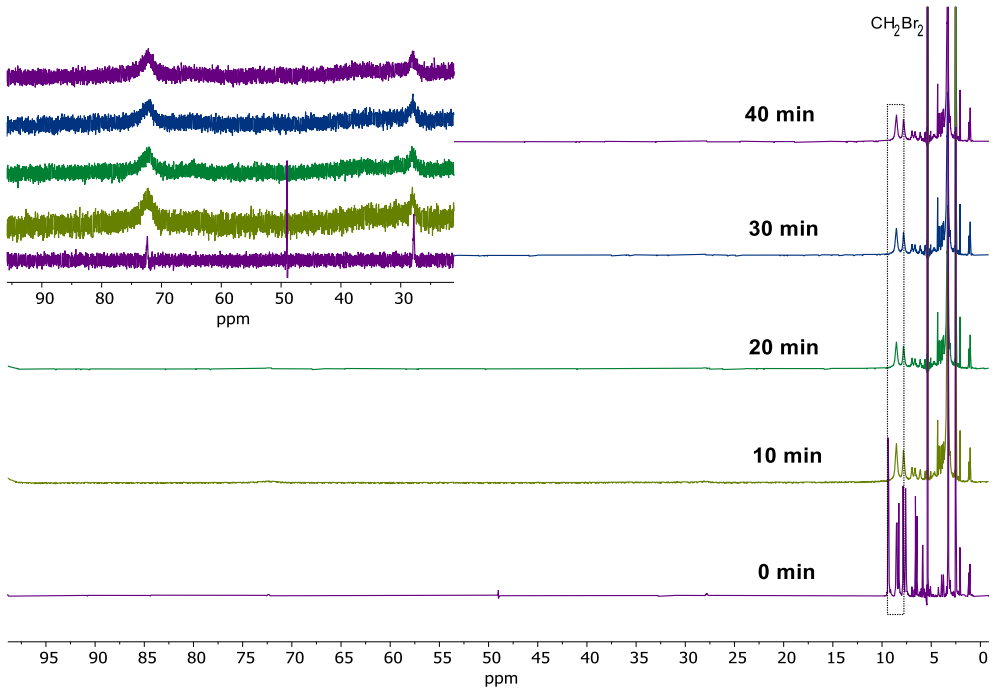

Figure S32. ^{1}H NMR spectra illustrating the dynamics of the reduction of the cobalt(III) complex [Co(**L**$^{\mathbf{Br}}$)$_2$(**esc**)]ClO$_4$ by ascorbic acid under argon at 40°C. The inset shows the paramagnetic region of the spectra featuring three signals from the protons of this complex with their intensities increasing with the reduction time.

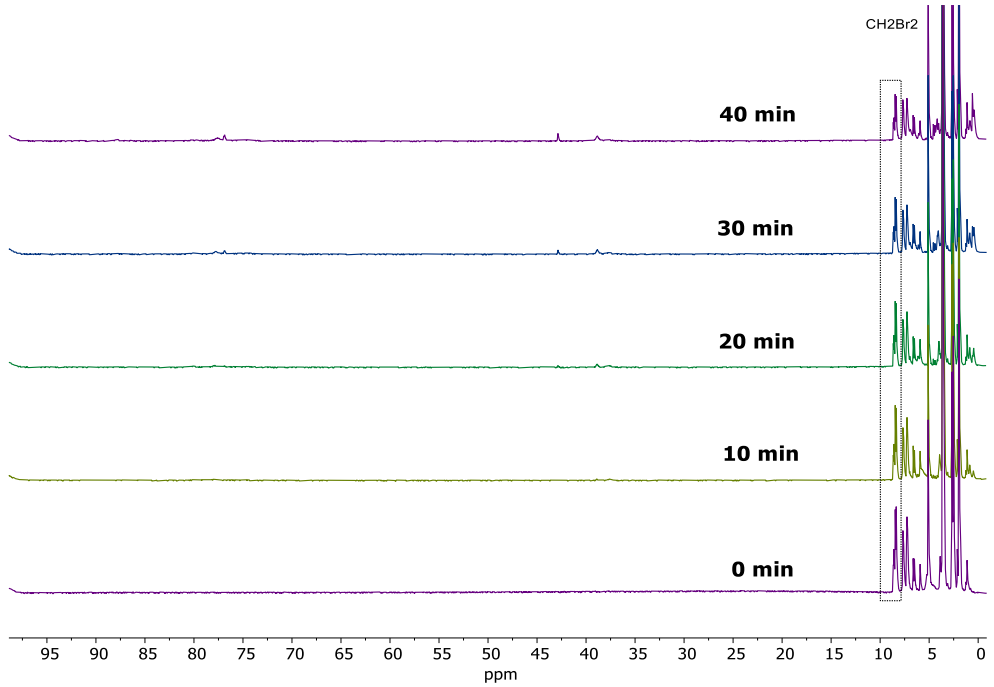

Figure S33. ^{1}H NMR spectra illustrating the dynamics of the reduction of the cobalt(III) complex [Co(**L**$^{\mathbf{Me}}$)$_2$(**esc**)]ClO$_4$ by ascorbic acid under argon at 40°C.

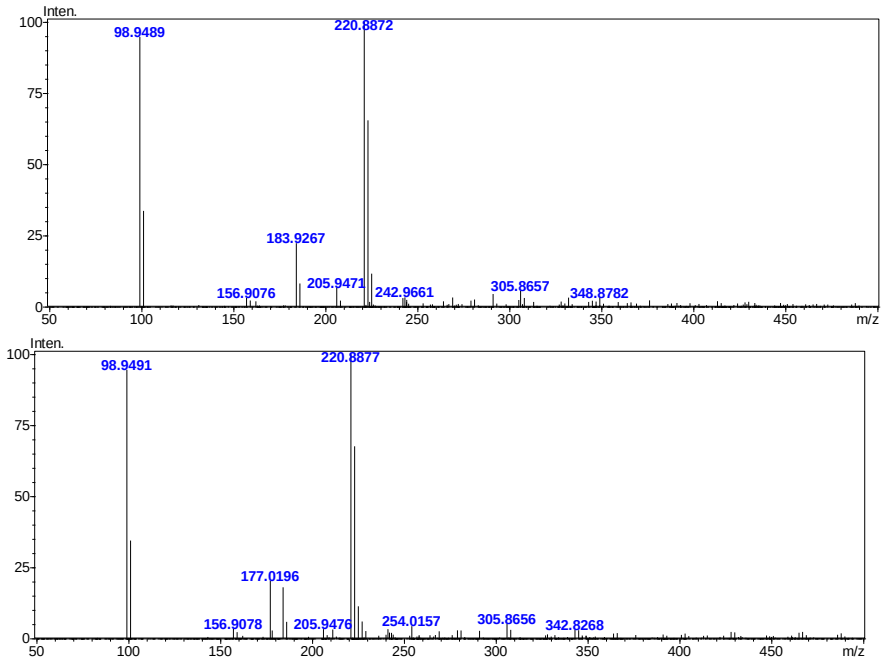

Figure S34. High-resolution mass spectra (negative ions) of the cobalt(III) complex [Co($\mathbf{L}^{\mathbf{OMe}}$)$_2$(**esc**)]ClO$_4$ (top) and of the reaction mixture with 2 eq. of ascorbic acid (bottom) after 1h under argon at 40^{o}C. Before the reduction, the mass-spectra featured no signals of esculetin, so the complex [Co($\mathbf{L}^{\mathbf{OMe}}$)$_2$(**esc**)]ClO$_4$ did not dissociate at the ionization conditions.

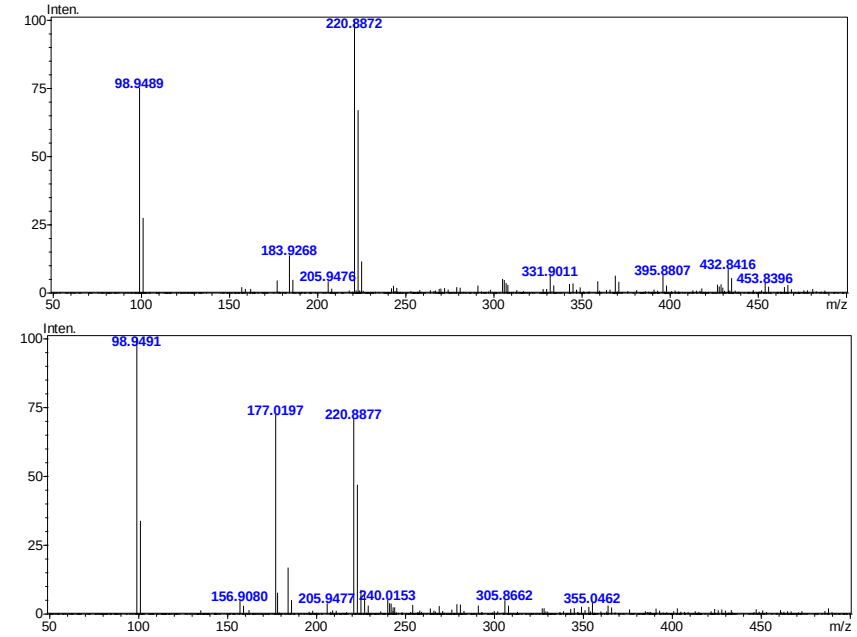

Figure S35. High-resolution mass spectra(negative ions) of the cobalt(III) complex [Co($\mathbf{L}^{\mathbf{COOMe}}$)$_2$(**esc**)]ClO$_4$ (top) and of the reaction mixture with 2 eq. of ascorbic acid (bottom) after 1h under argon at 40^{o}C. Before the reduction, the mass-spectra featured no signals of esculetin, so the complex [Co($\mathbf{L}^{\mathbf{COOMe}}$)$_2$(**esc**)]ClO$_4$ did not dissociate at the ionization conditions.

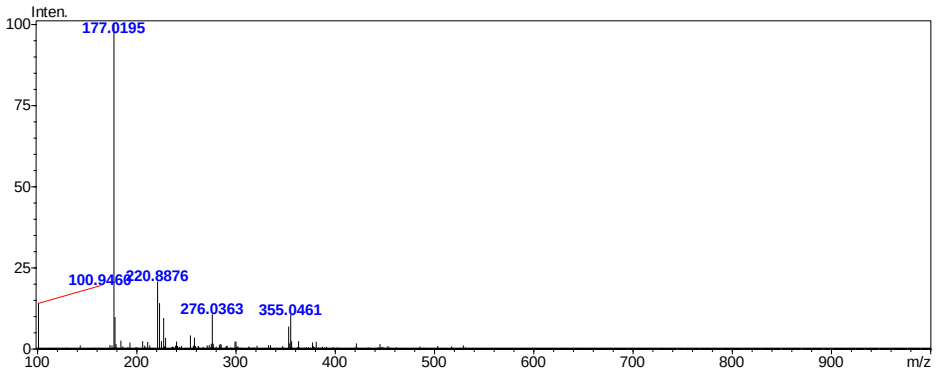

Figure S36. High-resolution mass spectrum (negative ions) of the precipitate that was isolated from the mixture of [Co(**L**$^{\mathbf{COOMe}}$)$_2$(**esc**)]ClO$_4$ with 2 eq. of ascorbic acid after 1h under argon at 40^{o}C and then dissolved in a mixture DMSO/CH$_3$CN (1:9 v/v).

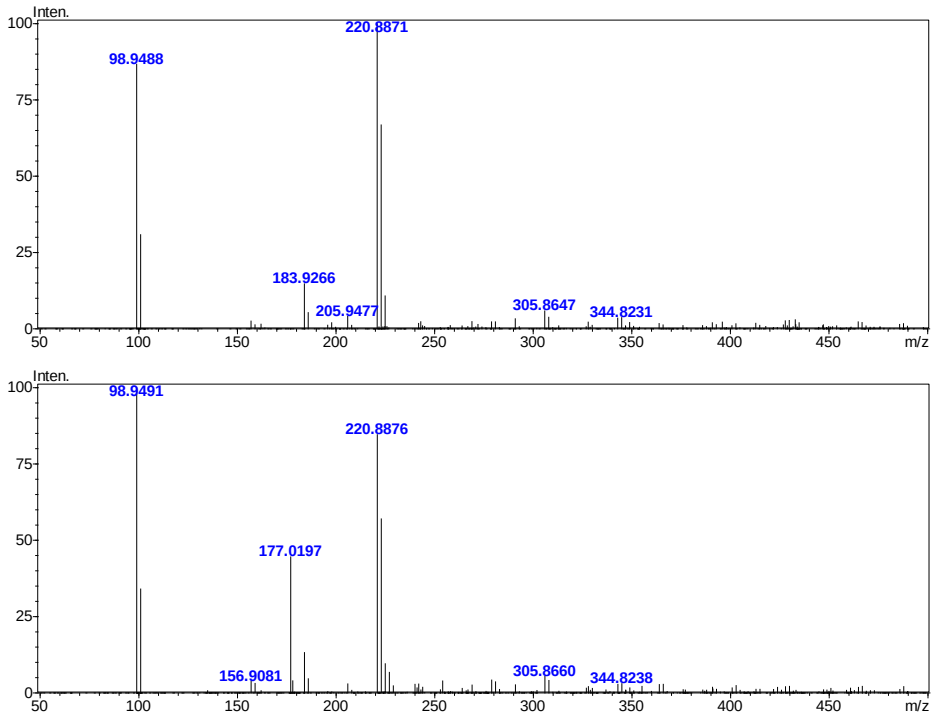

Figure S37. High-resolution mass spectra (negative ions) of the cobalt(III) complex [Co(**L**$^{\mathbf{H}}$)$_2$(**esc**)]ClO$_4$ (top) and of the reaction mixture with 2 eq. of ascorbic acid (bottom) after 1h under argon at 40^{o}C. Before the reduction, the mass-spectra featured no signals of esculetin, so the complex [Co(**L**$^{\mathbf{H}}$)$_2$(**esc**)]ClO$_4$ did not dissociate at the ionization conditions.

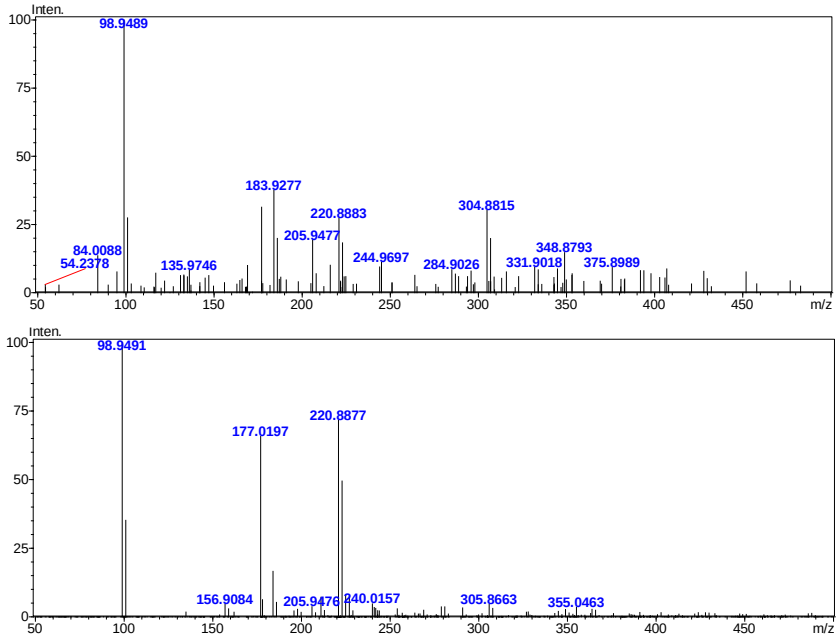

Figure S38. High-resolution mass spectrum (negative ions) of the cobalt(III) complex [Co($\mathbf{L}^{\mathbf{Cl}}$)$_2$(**esc**)]ClO_4 (top) and of the reaction mixture with 2 eq. of ascorbic acid (bottom) after 1h under argon at 40°C.

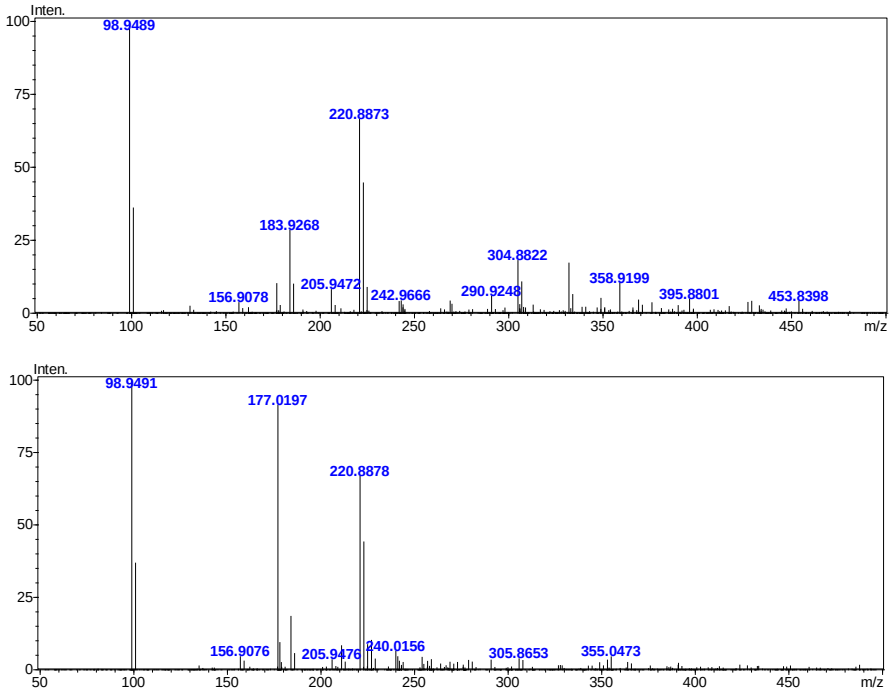

Figure S39. High-resolution mass spectra (negative ions) of the cobalt(III) complex [Co($\mathbf{L}^{\mathbf{Br}}$)$_2$(**esc**)]ClO_4 (top) and of the reaction mixture with 2 eq. of ascorbic acid (bottom) after 1h under argon at 40°C. Before the reduction, the mass-spectra featured no signals of esculetin, so the complex [Co($\mathbf{L}^{\mathbf{Br}}$)$_2$(**esc**)]ClO_4 did not dissociate at the ionization conditions.

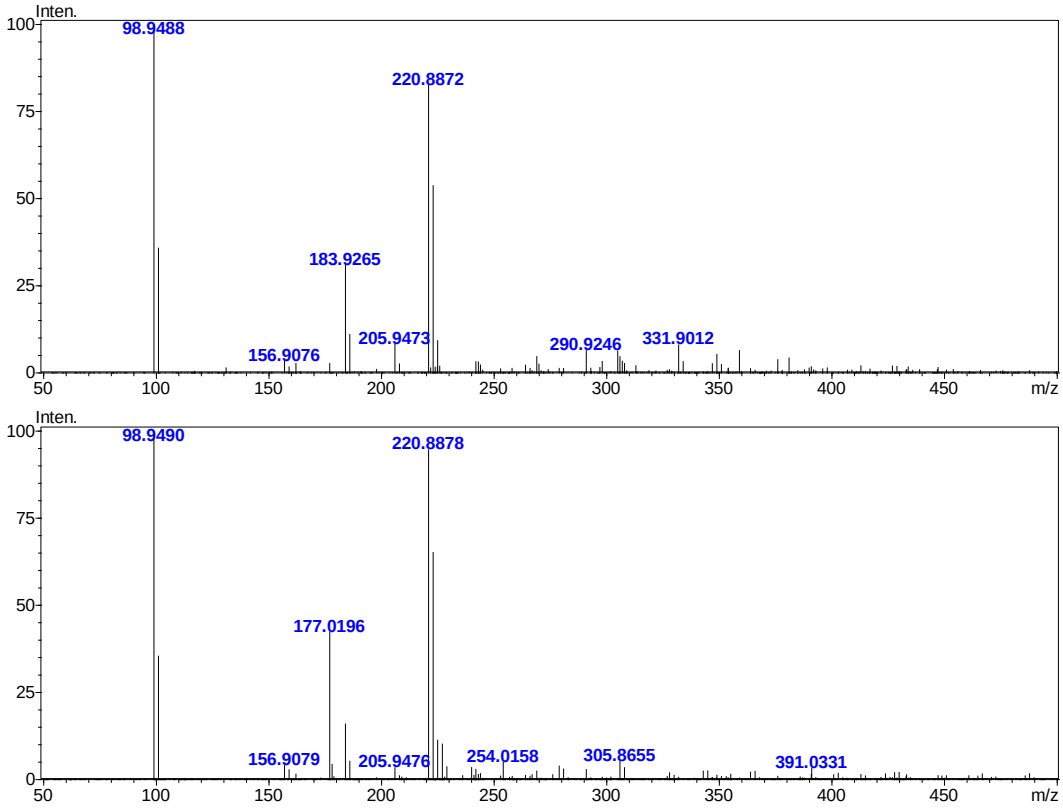

Figure S40. High-resolution mass spectra (negative ions) of the cobalt(III) complex [Co($\mathbf{L}^{\mathbf{Me}}$)$_2$(**esc**)]ClO_4 (top) and of the reaction mixture with 2 eq. of ascorbic acid (bottom) after 1h under argon at 40^{o}C. Before the reduction, the mass-spectra featured no signals of esculetin, so the complex [Co($\mathbf{L}^{\mathbf{Me}}$)$_2$(**esc**)]ClO_4 did not dissociate at the ionization conditions.

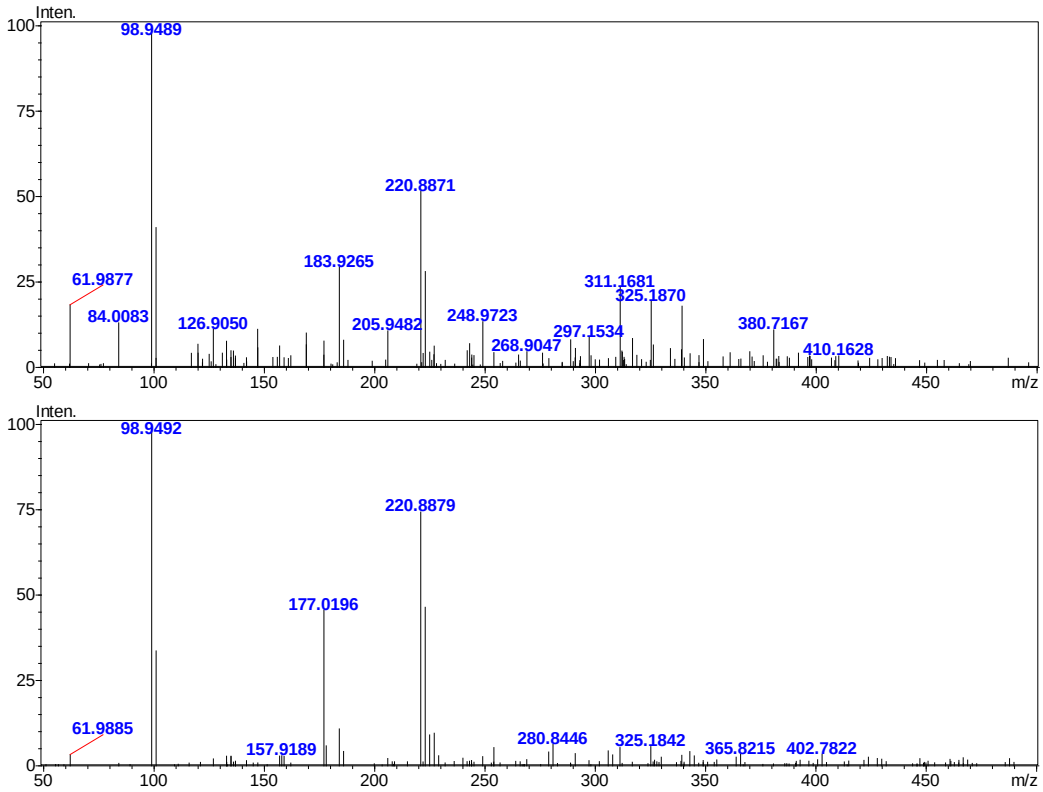

Figure S41. High-resolution mass spectra (negative ions) of the cobalt(III) complex [Co(**L**^{CH_2OH})$_2$(**esc**)]ClO$_4$ (top) and of the reaction mixture with 2 eq. of ascorbic acid (bottom) after 1h under argon at 40°C. Before the reduction, the mass-spectra featured no signals of esculetin, so the complex [Co(**L**^{CH_2OH})$_2$(**esc**)]ClO$_4$ did not dissociate at the ionization conditions.

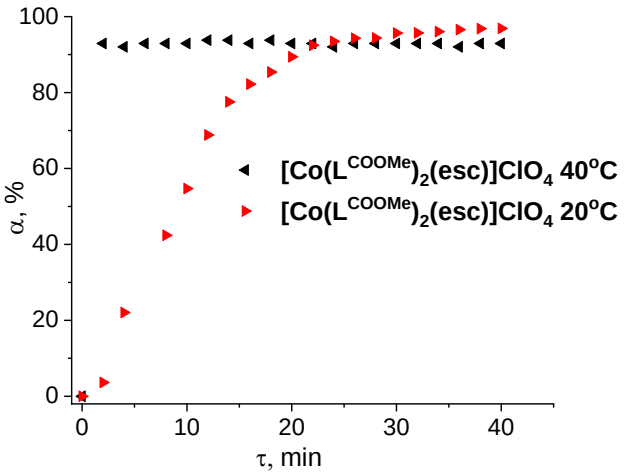

Figure S42. Conversion curves for the reduction of the cobalt(III) complex [Co(**L**^{COOMe})$_2$(**esc**)]ClO$_4$ by ascorbic acid under argon at 20 and 40°C.

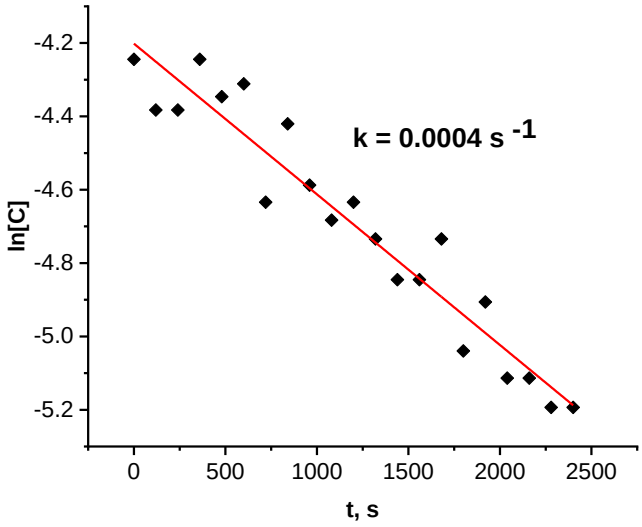

Figure S43. Kinetic curve for the reduction of the cobalt(III) complex [Co($\mathbf{L}^{\mathbf{OMe}}$)$_2$(**esc**)]ClO$_4$ in a mixture CD_3CN/D_2O by ascorbic acid under argon at 40°C. The red line corresponds to the best fit by a linear function.

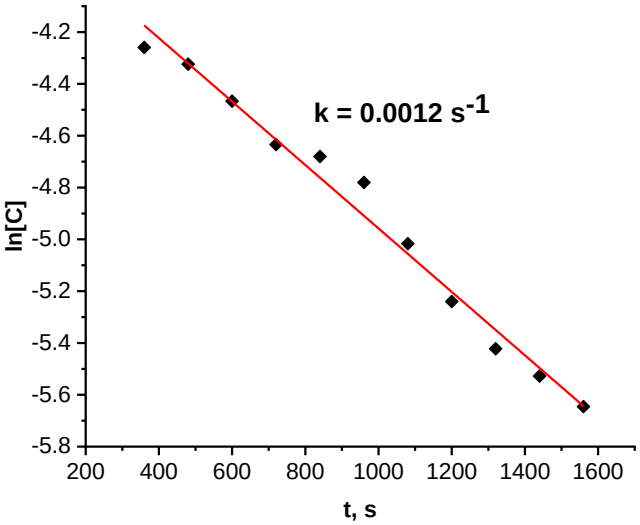

Figure S44. Kinetic curve for the reduction of the cobalt(III) complex [Co($\mathbf{L}^{\mathbf{H}}$)$_2$(**esc**)]ClO$_4$ in a mixture CD_3CN/D_2O by ascorbic acid under argon at 40°C. The red line corresponds to the best fit by a linear function.

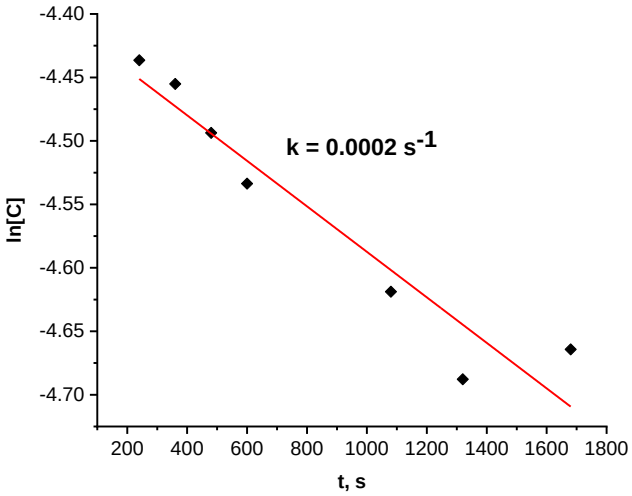

Figure S45. Kinetic curve for the reduction of the cobalt(III) complex [Co(**L**$^{\mathbf{Br}}$)$_2$(**esc**)]ClO$_4$ in a mixture DMSO-d$_6$/D$_2$O by ascorbic acid under argon at 40°C. The red line corresponds to the best fit by a linear function.

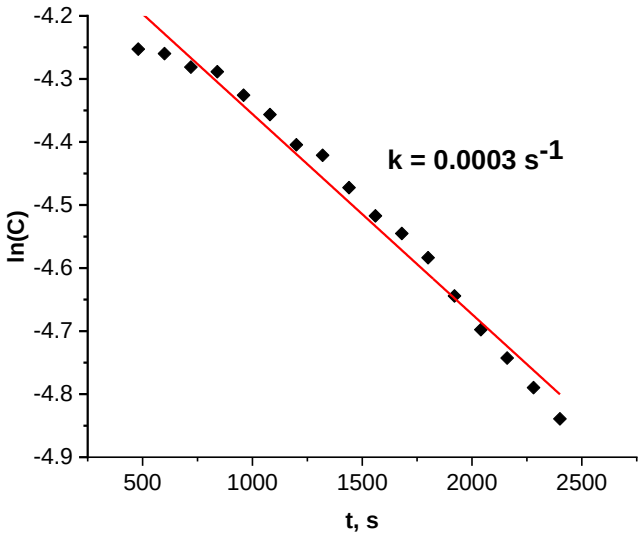

Figure S46. Kinetic curve for the reduction of the cobalt(III) complex [Co(**L**$^{\mathbf{Me}}$)$_2$(**esc**)]ClO$_4$ in a mixture CD$_3$CN/D$_2$O by ascorbic acid under argon at 40°C. The red line corresponds to the best fit by a linear function.

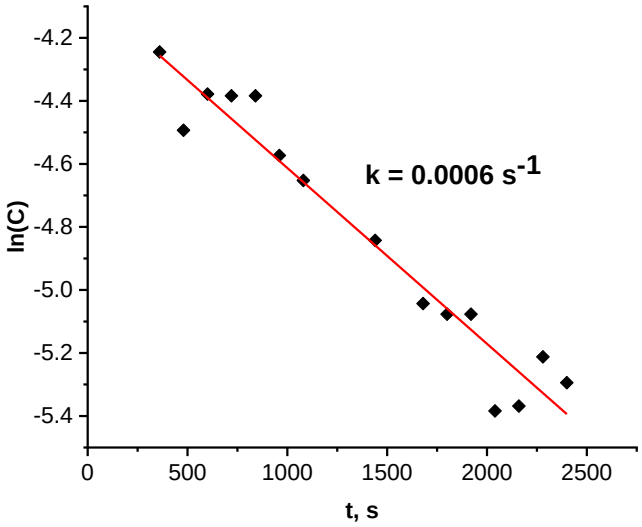

Figure S47. Kinetic curve for the reduction of the cobalt(III) complex [Co($\mathbf{L^{CH_2OH}}$)$_2$(**esc**)]ClO_4 in a mixture CD_3CN/D_2O by ascorbic acid under argon at 40°C. The red line corresponds to the best fit by a linear function.

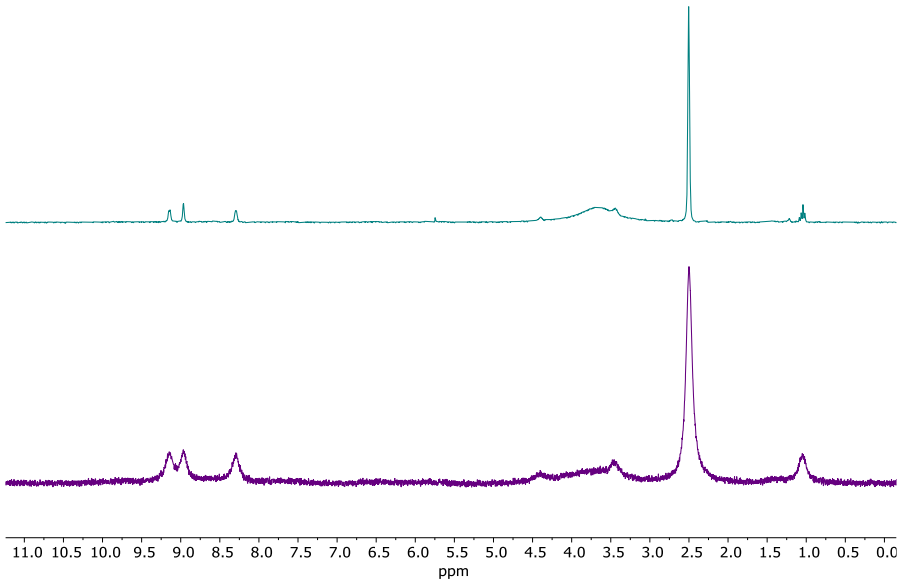

Figure S48. ^1H NMR spectra of $\mathbf{L^{NO_2}}$ (top) and of its mixture with cobalt(II) chloride (bottom) in DMSO-d_6. Broadening of the signals in the spectrum of the reaction mixture could be explained by the presence of paramagnetic species other than the target complex.

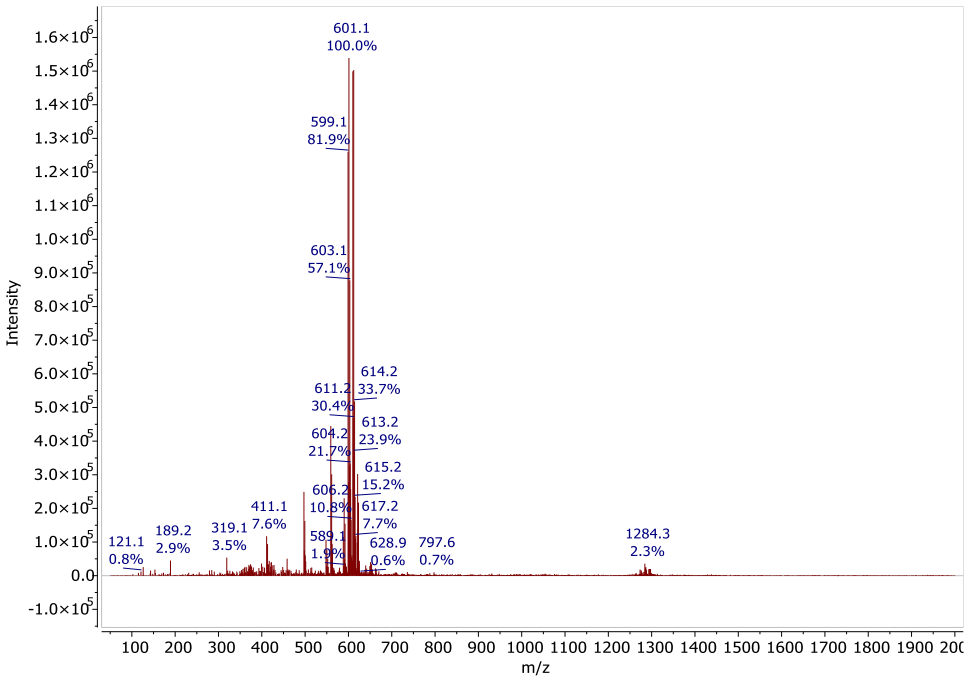

Figure S49. High-resolution mass spectra (positive ions) of the reaction mixture of $\mathbf{L^{NO_2}}$ and cobalt(II) chloride.

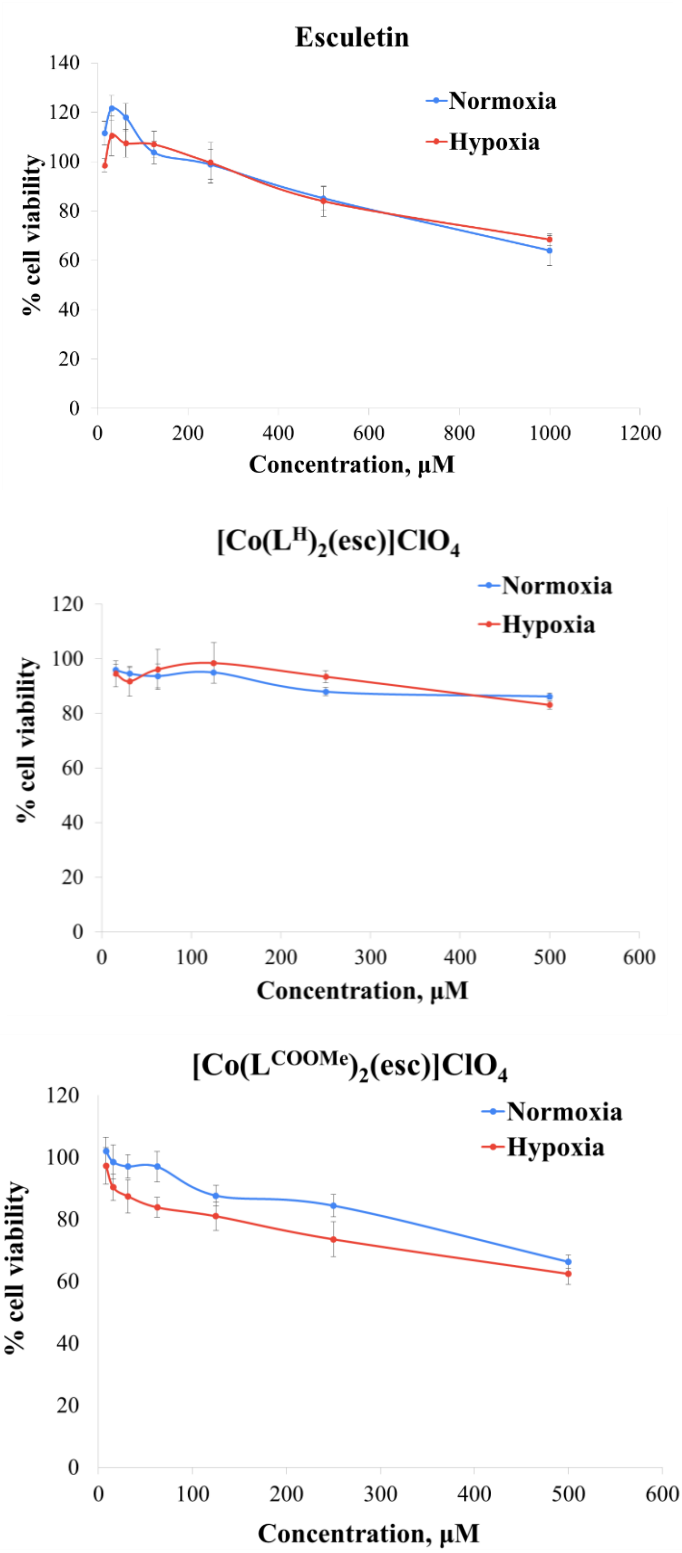

Figure S50. Cell viability of L929 cells (mean ± standard deviations from three independent experiments in triplicate) plotted *versus* the concentration of free esculetin, [Co(**L**$^{\mathbf{H}}$)$_2$(**esc**)]ClO$_4$ and [Co(**L**$^{\mathbf{COOMe}}$)$_2$(**esc**)]ClO$_4$. Hereinafter, blue lines correspond to normoxic conditions, and red lines, to hypoxic conditions.

Supplementary Tables:

Table S1. Composition of the mixture at the initial stage of the reduction of the cobalt(III) complex [Co(**L**$^{\mathbf{OMe}}$)$_2$(**esc**)]ClO$_4$ by ascorbic acid under argon at 40°C.

Molecular weight, g/mol	*Weight, mg*	*Concentration, M*	*Volume of CD_3CN, ml*	*Volume of D_2O, ml*	*Weight of ascorbic acid, mg*	*Volume of CH_2Br_2 (inner standard), µl*
766.88	7.7	0.0143	0.55	0.15	3.6	3

Table S2. Conversions (%) and ln[C] of the reduction of the cobalt(III) complex [Co(**L**$^{\mathbf{OMe}}$)$_2$(**esc**)]ClO$_4$ by ascorbic acid under argon at 40°C. Concentration C was estimated by multiplying % of the conversion by the initial concentration of the complex (see Table S1).

Time of reaction, s	*Integral intensity of the multiplet at 8.57-8.68 ppm in the NMR spectra (integral intensity of the signal from CH_2Br_2 is 1)*	*% from initial quantity of complex*	*% of conversion*	*ln[C]*
0	0.31	100	0	-4.244435046
120	0.27	87.09677419	12.90322581	-4.382585384
240	0.27	87.09677419	12.90322581	-4.382585384
360	0.31	100	0	-4.244435046
480	0.28	90.32258065	9.677419355	-4.34621774
600	0.29	93.5483871	6.451612903	-4.31112642
720	0.21	67.74193548	32.25806452	-4.633899813
840	0.26	83.87096774	16.12903226	-4.420325712
960	0.22	70.96774194	29.03225806	-4.587379797
1080	0.2	64.51612903	35.48387097	-4.682689977
1200	0.21	67.74193548	32.25806452	-4.633899813
1320	0.19	61.29032258	38.70967742	-4.733983271
1440	0.17	54.83870968	45.16129032	-4.845208906
1560	0.17	54.83870968	45.16129032	-4.845208906
1680	0.19	61.29032258	38.70967742	-4.733983271
1800	0.14	45.16129032	54.83870968	-5.039364921
1920	0.16	51.61290323	48.38709677	-4.905833528
2040	0.13	41.93548387	58.06451613	-5.113472893
2160	0.13	41.93548387	58.06451613	-5.113472893
2280	0.12	38.70967742	61.29032258	-5.193515601
2400	0.12	38.70967742	61.29032258	-5.193515601

Table S3. Composition of the mixture at the initial stage of the reduction of the cobalt(III) complex [Co(**L**$^{\mathbf{COOMe}}$)$_2$(**esc**)]ClO_4 by ascorbic acid under argon at 40°C.

Molecular weight, g/mol	*Weight, mg*	*Concentration, M*	*Volume of CD_3CN, ml*	*Volume of D_2O, ml*	*Weight of ascorbic acid, mg*	*Volume of CH_2Br_2 (inner standard), µl*
879.02	8.8	0.0143	0.55	0.15	3.8	3

Table S4. Conversions (%) and ln[C] of the reduction of the cobalt(III) complex [Co(**L**$^{\mathbf{COOMe}}$)$_2$(**esc**)]ClO_4 by ascorbic acid under argon at 40°C. Concentration C was estimated by multiplying % of the conversion by the initial concentration of the complex (see Table S3).

Time of reaction, s	*Integral intensity of the multiplet at 8.5-9.5 ppm in the NMR spectra (integral intensity of the signal from CH_2Br_2 is 1)*	*% from initial quantity of complex*	*% of conversion*	*ln[C]*
0	1.13	100	0	-4.368864043
120	0.08	7.079646018	92.92035398	-7.01681032
240	0.09	7.96460177	92.03539823	-6.899027284
360	0.08	7.079646018	92.92035398	-7.01681032
480	0.08	7.079646018	92.92035398	-7.01681032
600	0.08	7.079646018	92.92035398	-7.01681032
720	0.07	6.194690265	93.80530973	-7.150341713
840	0.07	6.194690265	93.80530973	-7.150341713
960	0.08	7.079646018	92.92035398	-7.01681032
1080	0.07	6.194690265	93.80530973	-7.150341713
1200	0.08	7.079646018	92.92035398	-7.01681032
1320	0.08	7.079646018	92.92035398	-7.01681032
1440	0.09	7.96460177	92.03539823	-6.899027284
1560	0.08	7.079646018	92.92035398	-7.01681032
1680	0.08	7.079646018	92.92035398	-7.01681032
1800	0.08	7.079646018	92.92035398	-7.01681032
1920	0.08	7.079646018	92.92035398	-7.01681032
2040	0.08	7.079646018	92.92035398	-7.01681032
2160	0.09	7.96460177	92.03539823	-6.899027284
2280	0.08	7.079646018	92.92035398	-7.01681032
2400	0.08	7.079646018	92.92035398	-7.01681032

Table S5. Composition of the mixture at the initial stage of the reduction of the cobalt(III) complex [Co(**L**$^{\mathbf{COOMe}}$)$_2$(**esc**)]ClO$_4$ by ascorbic acid under argon at 20°C.

Molecular weight, g/mol	*Weight, mg*	*Concentration, M*	*Volume of CD_3CN, ml*	*Volume of D_2O, ml*	*Weight of ascorbic acid, mg*	*Volume of CH_2Br_2 (inner standard), µl*
879.02	6.7	0.0126	0.4	0.2	2.8	3

Table S6. Conversions (%) and ln[C] of the reduction of the cobalt(III) complex [Co(**L**$^{\mathbf{COOMe}}$)$_2$(**esc**)]ClO$_4$ by ascorbic acid under argon at 20°C. Concentration C was estimated by multiplying % of the conversion by the initial concentration of the complex (see Table S5).

Time of reaction, s	*Integral intensity of the multiplet at 8.5-9.5 ppm in the NMR spectra (integral intensity of the signal from CH_2Br_2 is 1)*	*% from initial quantity of complex*	*% of conversion*	*ln[C]*
0	1.89	100.00	0.00	-4.368864043
120	1.82	96.36	3.64	-4.405905315
240	1.47	77.94	22.06	-4.618079835
480	1.09	57.61	42.39	-4.920360706
600	0.85	45.30	54.70	-5.160746064
720	0.59	31.18	68.82	-5.534370566
840	0.42	22.46	77.54	-5.862403934
960	0.34	17.79	82.21	-6.095665616
1080	0.28	14.60	85.40	-6.292974964
1200	0.20	10.60	89.40	-6.613180228
1320	0.14	7.54	92.46	-6.953929021
1440	0.12	6.54	93.46	-7.096840183
1560	0.11	5.69	94.31	-7.235904944
1680	0.11	5.63	94.37	-7.245515269
1800	0.08	4.33	95.67	-7.508451592
1920	0.08	4.30	95.70	-7.514966273
2040	0.07	3.96	96.04	-7.596755706
2160	0.07	3.45	96.55	-7.736810279
2280	0.06	3.17	96.83	-7.820347923
2400	0.06	3.11	96.89	-7.840478857

Table S7. Composition of the mixture at the initial stage of the reduction of the cobalt(III) complex $[Co(\mathbf{L^H})_2(\mathbf{esc})]ClO_4$ by ascorbic acid under argon at 40°C.

Molecular weight, g/mol	*Weight, mg*	*Concentration, M*	*Volume of CD_3CN, ml*	*Volume of D_2O, ml*	*Weight of ascorbic acid, mg*	*Volume of CH_2Br_2 (inner standard), µl*
646.88	6.4	0.0141	0.55	0.15	3.6	3

Table S8. Conversions (%) and ln[C] of the reduction of the cobalt(III) complex $[Co(\mathbf{L^H})_2(\mathbf{esc})]ClO_4$ by ascorbic acid under argon at 40°C. Concentration C was estimated by multiplying % of the conversion by the initial concentration of the complex (see Table S7).

Time of reaction, s	*Integral intensity of the multiplet at 8.79-8.88 ppm in the NMR spectra (integral intensity of the signal from CH_2Br_2 is 1)*	*% from initial quantity of complex*	*% of conversion*	*ln[C]*
0	0.32	100	0	-
120	0.32	100	0	-
240	0.32	100	0	-
360	0.32	100	0	-4.259187885
480	0.3	93.75	6.25	-4.323726406
600	0.26	81.25	18.75	-4.46682725
720	0.22	68.75	31.25	-4.633881335
840	0.21	65.625	34.375	-4.68040135
960	0.19	59.375	40.625	-4.780484809
1080	0.15	46.875	53.125	-5.016873587
1200	0.12	37.5	62.5	-5.240017138
1320	0.1	31.25	68.75	-5.422338695
1440	0.09	28.125	71.875	-5.527699211
1560	0.08	25	75	-5.645482246
1680	0.08	25	75	-
1800	0.08	25	75	-
1920	0.08	25	75	-
2040	0.08	25	75	-
2160	0.08	25	75	-
2280	0.08	25	75	-
2400	0.08	25	75	-

Table S9. Composition of the mixture at the initial stage of the reduction of the cobalt(III) complex $[Co(\mathbf{L^H})_2(\mathbf{esc})]ClO_4$ by ascorbic acid under argon at 40°C.

Molecular weight, g/mol	*Weight, mg*	*Concentration, M*	*Volume of DMSO-d6, ml*	*Volume of D_2O, ml*	*Weight of ascorbic acid, mg*	*Volume of CH_2Br_2 (inner standard), µl*
784.66	7.8	0.0142	0.550	0.150	3.8	3

Table S10. Conversions (%) and ln[C] of the reduction of the cobalt(III) complex $[Co(\mathbf{L^{Cl}})_2(\mathbf{esc})]ClO_4$ by ascorbic acid. Concentration C was estimated by multiplying % of the conversion by the initial concentration of the complex (see Table S9).

Time of reaction, s	*Integral intensity of the multiplet at 8.04-8.74 ppm in the NMR spectra (integral intensity of the signal from CH_2Br_2 is 1)*	*% from initial quantity of complex*	*% of conversion*	*ln[C]*
0	0.53	100	0	
120	0.4	75.47169811	24.52830189	-4.535864297
240	0.37	69.81132075	30.18867925	
360	0.39	73.58490566	26.41509434	-4.561182105
480	0.36	67.9245283	32.0754717	
600	0.37	69.81132075	30.18867925	
720	0.38	71.69811321	28.30188679	-4.587157591
840	0.38	71.69811321	28.30188679	-4.587157591
960	0.37	69.81132075	30.18867925	-4.613825838
1200	0.34	64.1509434	35.8490566	
1320	0.36	67.9245283	32.0754717	-4.641224812
1440	0.36	67.9245283	32.0754717	-4.641224812
1560	0.36	67.9245283	32.0754717	
1680	0.36	67.9245283	32.0754717	
1800	0.35	66.03773585	33.96226415	-4.669395689
1920	0.35	66.03773585	33.96226415	
2040	0.37	69.81132075	30.18867925	
2160	0.34	64.1509434	35.8490566	-4.698383226
2280	0.32	60.37735849	39.62264151	
2400	0.34	64.1509434	35.8490566	

Table S11. Composition of the mixture at the initial stage of the reduction of the cobalt(III) complex [Co(**L**$^{\mathbf{H}}$)$_2$(**esc**)]ClO$_4$ by ascorbic acid under argon at 40ºC.

Molecular weight, g/mol	*Weight, mg*	*Concentration, M*	*Volume of DMSO-d6, ml*	*Volume of D_2O, ml*	*Weight of ascorbic acid, mg*	*Volume of CH_2Br_2 (inner standard), µl*
962.46	9.6	0.0142	0.550	0.150	3.8	3

Table S12. Conversions (%) and ln[C] of the reduction of the cobalt(III) complex [Co(**L**$^{\mathbf{Br}}$)$_2$(**esc**)]ClO$_4$ by ascorbic acid. Concentration C was estimated by multiplying % of the conversion by the initial concentration of the complex (see Table S11).

Time of reaction, s	*Integral intensity of the multiplet at 7.99-8.83 ppm in the NMR spectra (integral intensity of the signal from CH_2Br_2 is 1)*	*% from initial quantity of complex*	*% of conversion*	*ln[C]*
0	0.65	100	0	
240	0.54	83.07692308	16.92307692	-4.436457667
360	0.53	81.53846154	18.46153846	-4.4551498
480	0.51	78.46153846	21.53846154	-4.493616081
600	0.49	75.38461538	24.61538462	-4.533621416
720	0.47	72.30769231	27.69230769	
840	0.45	69.23076923	30.76923077	
960	0.48	73.84615385	26.15384615	
1080	0.45	69.23076923	30.76923077	-4.618779224
1200	0.43	66.15384615	33.84615385	
1320	0.42	64.61538462	35.38461538	-4.687772096
1440	0.45	69.23076923	30.76923077	
1560	0.41	63.07692308	36.92307692	
1680	0.43	66.15384615	33.84615385	-4.664241598
1800	0.42	64.61538462	35.38461538	
1920	0.42	64.61538462	35.38461538	
2040	0.42	64.61538462	35.38461538	
2160	0.43	66.15384615	33.84615385	
2400	0.41	63.07692308	36.92307692	

Table S13. Composition of the mixture at the initial stage of the reduction of the cobalt(III) complex $[Co(\mathbf{L^{Me}})_2(\mathbf{esc})]ClO_4$ by ascorbic acid under argon at 40°C.

Molecular weight, g/mol	*Weight , mg*	*Concentration, M*	*Volume of CD_3CN, ml*	*Volume of D_2O, ml*	*Weight of ascorbic acid, mg*	*Volume of CH_2Br_2 (inner standard), µl*
702.98	7.0	0.0142	0.550	0.150	3.8	3

Table S14. Conversions (%) and ln[C] of the reduction of the cobalt(III) complex $[Co(\mathbf{L^{Me}})_2(\mathbf{esc})]ClO_4$ by ascorbic acid under argon at 40°C. Concentration C was estimated by multiplying % of the conversion by the initial concentration of the complex (see Table S13).

Time of reaction, s	*Integral intensity of the multiplet at 8.34-8.63 ppm in the NMR spectra (integral intensity of the signal from CH_2Br_2 is 1)*	*% from initial quantity of complex*	*% of conversion*	*ln[C]*
0	1.19	83.8028169	16.1971831	
120	1.13	79.57746479	20.42253521	
240	1.27	89.43661972	10.56338028	
360	1.32	92.95774648	7.042253521	
480	1.42	100	0	-4.252743332
600	1.41	99.29577465	0.704225352	-4.2598105
720	1.38	97.18309859	2.816901408	-4.281316705
840	1.37	96.47887324	3.521126761	-4.288589464
960	1.32	92.95774648	7.042253521	-4.325768467
1080	1.28	90.14084507	9.85915493	-4.356540126
1200	1.22	85.91549296	14.08450704	-4.404549345
1320	1.2	84.50704225	15.49295775	-4.421078647
1440	1.14	80.28169014	19.71830986	-4.472371942
1560	1.09	76.76056338	23.23943662	-4.517222508
1680	1.06	74.64788732	25.35211268	-4.545131296
1800	1.02	71.83098592	28.16901408	-4.583597577
1920	0.96	67.6056338	32.3943662	-4.644222199
2040	0.91	64.08450704	35.91549296	-4.697710884
2160	0.87	61.26760563	38.73239437	-4.742662271
2280	0.83	58.45070423	41.54929577	-4.789729782
2400	0.79	55.63380282	44.36619718	-4.839122538

TableS15. Composition of the mixture at the initial stage of the reduction of the cobalt(III) complex [Co(**L**$^{\mathbf{CH_2OH}}$)$_2$(**esc**)]ClO_4 by ascorbic acid under argon at 40°C.

Molecular weight, g/mol	*Weight, mg*	*Concentration, M*	*Volume of CD_3CN, ml*	*Volume of D_2O, ml*	*Weight of ascorbic acid, mg*	*Volume of CH_2Br_2 (inner standard), µl*
766.98	7.7	0.143	0.55	0.15	3.8	3

Table S16. Conversions (%) and ln[C] of the reduction of the cobalt(III) complex [Co(**L**$^{\mathbf{CH_2OH}}$)$_2$(**esc**)]ClO_4 by ascorbic acid under argon at 40°C. Concentration C was estimated by multiplying % of the conversion by the initial concentration of the complex (see Table S15).

Time of reaction, s	*Integral intensity of the multiplet at 8.50-8.77 ppm in the NMR spectra (integral intensity of the signal from CH_2Br_2 is 1)*	*% from initial quantity of complex*	*% of conversion*	*ln[C]*
0	0.93	46.5	53.5	
120	1.61	80.5	19.5	
240	1.77	88.5	11.5	
360	2	100	0	-4.24
480	1.56	78	22	-4.49
600	1.75	87.5	12.5	-4.38
720	1.74	87	13	-4.38
840	1.74	87	13	-4.38
960	1.44	72	28	-4.57
1080	1.33	66.5	33.5	-4.65
1200	1.34	67	33	
1320	1.29	64.5	35.5	
1440	1.1	55	45	-4.84
1560	1.15	57.5	42.5	
1680	0.9	45	55	-5.04
1800	0.87	43.5	56.5	-5.08
1920	0.87	43.5	56.5	-5.08
2040	0.64	32	68	-5.38
2160	0.65	32.5	67.5	-5.37
2280	0.76	38	62	-5.21
2400	0.7	35	65	-5.29